



OPEN ACCESS

EDITED BY

Yuanyuan Feng,
Shanghai Jiao Tong University, China

REVIEWED BY

Alison Elizabeth Murray,
Desert Research Institute (DRI),
United States
Susanne Neuer,
Arizona State University, United States

*CORRESPONDENCE

Magda G. Cardozo-Mino
✉ mcardozo@mpi-bremen.de
Christina Bienhold
✉ christina.bienhold@awi.de

†PRESENT ADDRESS

Ian Salter,
Environment Department,
Faroe Marine Research Institute,
Tórshavn, Faroe Islands

RECEIVED 24 February 2023

ACCEPTED 16 June 2023

PUBLISHED 11 July 2023

CITATION

Cardozo-Mino MG, Salter I, Nöthig E-M,
Metfies K, Ramondenc S, Wekerle C,
Krumpfen T, Boetius A and Bienhold C
(2023) A decade of microbial
community dynamics on sinking
particles during high carbon export
events in the eastern Fram Strait.
Front. Mar. Sci. 10:1173384.
doi: 10.3389/fmars.2023.1173384

COPYRIGHT

© 2023 Cardozo-Mino, Salter, Nöthig,
Metfies, Ramondenc, Wekerle, Krumpfen,
Boetius and Bienhold. This is an open-access
article distributed under the terms of the
[Creative Commons Attribution License
\(CC BY\)](https://creativecommons.org/licenses/by/4.0/). The use, distribution or
reproduction in other forums is permitted,
provided the original author(s) and the
copyright owner(s) are credited and that
the original publication in this journal is
cited, in accordance with accepted
academic practice. No use, distribution or
reproduction is permitted which does not
comply with these terms.

A decade of microbial community dynamics on sinking particles during high carbon export events in the eastern Fram Strait

Magda G. Cardozo-Mino^{1,2,3*}, Ian Salter^{2†}, Eva-Maria Nöthig⁴,
Katja Metfies⁴, Simon Ramondenc², Claudia Wekerle⁵,
Thomas Krumpfen⁶, Antje Boetius^{1,2,7} and Christina Bienhold^{1,2*}

¹HGF-MPG Group for Deep Sea Ecology and Technology, Max Planck Institute for Marine Microbiology, Bremen, Germany, ²HGF-MPG Group for Deep Sea Ecology and Technology, Alfred Wegener Institute Helmholtz Center for Polar and Marine Research, Bremerhaven, Germany, ³Faculty of Geosciences, University of Bremen, Bremen, Germany, ⁴Polar Biological Oceanography, Alfred Wegener Institute Helmholtz Center for Polar and Marine Research, Bremerhaven, Germany, ⁵Physical Oceanography, Alfred Wegener Institute Helmholtz Center for Polar and Marine Research, Bremerhaven, Germany, ⁶Sea Ice Physics, Alfred Wegener Institute Helmholtz Center for Polar and Marine Research, Bremerhaven, Germany, ⁷MARUM Center for Marine Environmental Sciences, University of Bremen, Bremen, Germany

Marine sinking particles sequester atmospheric carbon dioxide to the deep ocean via the biological carbon pump. Understanding how environmental shifts drive changes in the microbial composition of particles, and how these affect the export of organic matter from the surface to the deep ocean, is critical, especially in the rapidly changing Arctic Ocean. Here, we applied next generation sequencing of the 18S and 16S rRNA genes to sediment trap samples from around 200 m water depth in the eastern Fram Strait, covering a time frame of more than one decade (2000–2012). The aim was to characterize their microbial composition during annual highest particulate organic carbon flux events. The bimodal annual spring and summer export fluxes were representative of the strong seasonality in the region. Furthermore, the study period was characterized by considerable interannual variation, marked especially by a warm water anomaly between 2005 and 2007. During this period changes in the hydrography and sea ice cover also led to measurable changes in the microbial composition of particles. The warm water period was marked by a decrease in diatoms affiliated with *Chaetoceros*, an increase of small phytoplankton and an increase in sequence abundance of the bacterial taxa *Oceanospirillales*, *Alteromonadales* and *Rhodobacterales* on the particles. The resulting changes in microbial composition and the associated microbial network structure suggest the emergence of a more developed retention system in the surface ocean. Our results provide the first long-term assessment of the microbial composition of sinking particles in the Arctic Ocean, and stress the importance of sea ice and hydrography for particle composition and subsequent flux of organic matter to deeper waters.

KEYWORDS

Arctic Ocean, marine sinking particles, amplicon sequencing, sea ice, warm anomaly, Atlantic water, time series

1 Introduction

Sinking particles play a key role in the global carbon cycle by transporting particulate organic matter (POM) from the surface to deeper ocean layers in a process called the biological carbon pump (BCP) (De La Rocha and Passow, 2007; Turner, 2015; Iversen, 2023). A large proportion of the sinking particles originate in the photic zone from primary production, either directly by aggregating phytoplankton, or by grazing. The particles consist of live and dead phytoplankton, zooplankton and bacterioplankton, as well as inorganic components such as mineral grains, zooplankton shells other ballast minerals (calcium carbonate, opal, and lithogenic material), and fecal matter (Alldredge and Silver, 1988; Simon et al., 2002; Jiao et al., 2010; Turner, 2015; Cruz et al., 2021). Particle composition is strongly determined by the plankton communities and environmental conditions in surface waters where the particles are formed (Simon et al., 2002; Buesseler and Boyd, 2009; Guidi et al., 2009; Bach et al., 2016).

Sinking particles act as “hot spots” of microbial diversity and activity (Azam and Malfatti, 2007). The microbial communities that colonize particles play a key role in the degradation of particulate organic carbon (POC) (Alldredge and Silver, 1988; Grossart et al., 2003; Fontanez et al., 2015), with implications for food web structures, export efficiency (Ducklow et al., 2001), and the flux of nutrients and carbon to deeper water layers (Simon et al., 2002; Iversen and Ploug, 2010; Grabowski et al., 2019). The activity of heterotrophic microbes determines particle remineralization rates across different depth layers of the ocean (Datta et al., 2016). In addition, sinking particles can act as dispersal vectors of viable microbial communities from the surface to the deep ocean (Mestre et al., 2018; Preston et al., 2020; Ruiz-González et al., 2020; Fadeev et al., 2021b), thus influencing the microbial structure and functioning of the deep sea (Gibbons et al., 2013; Cram et al., 2015; Thiele et al., 2015; Rapp et al., 2018). Recent studies have addressed molecular microbial community composition of sinking particles across seasons in other oceanographic regions (Boeuf et al., 2019; Preston et al., 2020), and the need to further observation thereof (Claustre et al., 2021). This study focuses for the first time on sinking particle-associated microbial community dynamics over multiyear time scales to assess effects of long-term environmental changes on microbial dynamics and POC export in the Fram Strait, Arctic Ocean.

The Arctic Ocean is one of the most rapidly changing areas of the world, with increases in temperature 4 times faster than the global average comparing the past 40 years (Rantanen et al., 2022). Substantial decreases in sea ice extent and thickness (Stroeve and Notz, 2018) are some of the most prominent manifestations of global warming today (Peng and Meier, 2018; Dai et al., 2019; Lannuzel et al., 2020). These environmental changes already have strong impacts on the pelagic system, including increases in primary production across shelf seas of the Arctic Ocean (Arrigo et al., 2012; Lewis et al., 2020; Nöthig et al., 2020). Arctic warming and sea ice retreat alters pelagic species composition (Leu et al., 2011; Nöthig et al., 2015; Hop et al., 2019), the composition and structure of sinking particles, fecal pellets and marine snow exported to the seafloor (Wassmann and Reigstad, 2011; Boetius

et al., 2013; Wiedmann et al., 2020), and may weaken pelagic-benthic coupling as sea ice continues to retreat (Fadeev et al., 2021b).

Fram Strait, which is located between Greenland and Spitsbergen (Figure 1), is the main gateway between the Atlantic and Arctic Ocean. It is a hydrographically complex area with two dynamic current systems, the East Greenland Current (EGC) that transports sea ice with the Transpolar Drift out of the Arctic and the West Spitsbergen Current (WSC) that feeds Atlantic water into the Arctic Ocean (Beszczynska-Moeller et al., 2011). Over the past decades, the eastern Fram Strait has seen increased heat flux in the WSC (Walczowski et al., 2017). A particular event was a warm water anomaly (WWA) that occurred between 2005 and 2007 (Beszczynska-Möller et al., 2012). At the same time, winter sea ice export through Fram Strait amplified over the past decades as a result of warming-induced increased Transpolar Drift velocity (Krumpfen et al., 2019). Moreover, sea-ice transport from the central Arctic to the Atlantic Ocean *via* Fram Strait and the Transpolar Drift is influenced by the Arctic dipole pressure anomaly (Krumpfen et al., 2019). These changes have been accompanied by shifts in the timing and composition of phytoplankton blooms and zooplankton occurrences (Weydmann et al., 2014; Busch et al., 2015; Nöthig et al., 2015; Soltwedel et al., 2016; Schröter et al., 2019; Ramondenc et al., 2022). e.g., with a transition from diatom- to flagellate-dominated summer phytoplankton communities (Nöthig et al., 2015). This changes the composition of particle export fluxes (Bauerfeind et al., 2009; Lalonde et al., 2011; Lalonde et al., 2013), and the migration behavior of main zooplankton species with consequences for higher trophic levels (Ramondenc et al., 2022). Only recently, Fadeev et al. (2021b) observed a decline in particle size and sinking rates in ice-free compared to ice-covered areas of Fram Strait, and hypothesized weakening of pelagic-benthic coupling and vertical microbial connectivity as sea ice continues to retreat. Another study in the same area evidenced measurable impacts of variations in sea ice derived meltwater stratification on the biological carbon pump (von Appen et al., 2021). However, it remains largely unknown if, or how, the changes in sea ice cover, hydrography and pelagic community composition affect the microbial composition of sinking particles, especially over long timescales.

Here, in the framework of the Long-Term Ecological Research (LTER) observatory HAUSGARTEN (78.5°N - 80°N, 05°W - 11°E), we utilized a bio-archive of moored sediment trap samples to compare interannual shifts in microbial eukaryotic and bacterial community composition between 2000 and 2012. We selected those samples with the highest POC export fluxes (HPF) during spring and summer in each year, and analyzed their molecular community composition in context of the prevailing environmental conditions. We tested the hypotheses that 1) spring (March to May) and summer (June to September) export events differ in microbial composition, according to the seasonal development of the ecosystem, 2) interannual differences in community composition are linked to environmental shifts in the region, and that 3) changes in community composition may be linked to differences in peak POC export.

2 Materials and methods

2.1 Sample collection

Sinking particles were sampled with Kiel type sediment traps (K.U.M. trap type K/MT 234, Kiel Germany) with a sampling area of 0.5 m² and 20 liquid-tight sampling cups, deployed and recovered yearly from 2000 to 2012 at the central LTER HAUSGARTEN station HGIV (~79.01N, ~4.20E). An electronic failure of the sediment trap prevented the collection of sinking material during the 2003-2004 operational year and from mid-March through July 2002. The depth of the sediment traps ranged between 179 m and 280 m (only one sediment trap from July 2009 to July 2010 was deployed at 80 m) with an average deployment depth of 200 m over the study period, i.e. traps were at all times below the mixed layer in spring and summer. The sample cups were programmed to collect in intervals of 7 to 31 days depending on the predicted timing of the productive season and POC flux. Sampling cups were filled with filtered North Sea seawater adjusted to a salinity of 40 PSU with NaCl, and poisoned with HgCl₂ to a final concentration of 0.14%. After recovery, the samples were refrigerated until further processing in the laboratory. Before splitting of the samples, zooplankton (swimmers) with a size larger than 0.5 mm were carefully picked with forceps under a dissecting microscope at a magnification of 20 and 50. The samples were split by a wet splitting procedure as described by von

Bodungen et al. (1991) and stored as 1/8 volumetric splits in their original preservative at 4°C. For this study we selected samples with the highest POC fluxes in each year. We identified a few samples that had shown signs of decomposition in the original cups and were thus rated unsuited for further analyses. Five samples showed signs of decomposition, regardless of the time of storage which varied from 3 to 15 years (in summer 2002, spring 2003, summer 2004 and in spring 2007), and were removed from the data set. Signs of decomposition observed shortly after recovery of the samples included rotten and sulfidic smell, black color, and signs of zooplankton decomposition, indicating incomplete fixation in the cups after sample collection. The POC flux of the 5 samples varied from 9 to 50 mg m⁻² d⁻¹ and did not coincide with the highest POC flux values in the dataset.

2.2 Biogenic fluxes

Particulate flux measurements were retrieved from the Data Publisher for Earth & Environmental Science PANGAEA (www.pangaea.de; Table S2). Methods are briefly described here. Subsamples for the analysis of total sedimented matter in dry weight (DW), and biogenic material (POC, particulate organic nitrogen PON, calcium carbonate CaCO₃, and particulate biogenic silica Si) were filtered, and analyzed as described by (Bodungen et al., 1991). Subsamples for POC measurements were filtered on pre-weighted

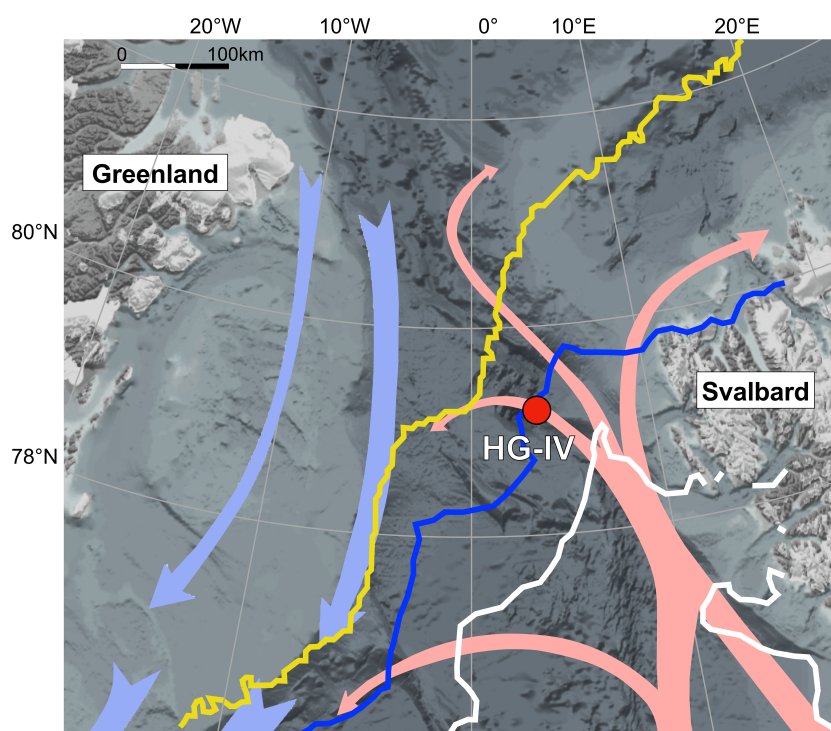


FIGURE 1

Map of the Fram Strait area depicting the deployment location (~79.01°N, ~4.20°E) of the sediment traps at the central station (HG-IV) of the HAUSGARTEN observatory from 2000 to 2012. The red arrows indicate the West Spitsbergen Current carrying Atlantic Water into the region and the blue arrow the East Greenland Current with cold polar water exiting the Arctic Ocean. To visualize sea ice variations, the monthly median sea ice edge is depicted for June 2000 in white, June 2006 (peak of the WWA) in dark blue and June 2012 (last sampling date, 2012 was also the lowest sea ice minimum extent recorded to date) in bright yellow. Visualization and sea ice data were obtained from <https://maps.awi.de> (Grosfeld et al., 2016).

GF/F filter with a pore size of 0.7 μm and pre-combusted at 500°C for 4 h. POC filters were soaked in 0.1 N HCL to remove inorganic carbon, and dried at 60°C (Lalande et al., 2013; Lalande et al., 2014). POC was measured using an elemental CHN analyzer (Lalande et al., 2013). The total flux and the CaCO_3 flux were corrected when organisms containing calcium carbonate, such as pteropods, were present in the sample. The corrections were done by applying a factor of 0.174 mg/ind for DW and 0.167 mg/ind for carbonate (Bauerfeind et al., 2009). Subsamples for Si were filtered on cellulose acetate filters with a pore size of 0.8 μm , measurements were obtained by wet-alkaline digestion of the samples and extracted for 2 h at 85°C in a shaking water bath (Bodungen et al., 1991).

2.3 Sediment trap catchment area and remote sensing data

The upper ocean can experience physical factors contributing to the displacement of particles from their place of production during sinking, among those mesoscale eddies, and lateral advection, with magnitudes of their effects also depending on particle settling velocities (Wanik et al., 2005; Waite et al., 2016). Estimating the catchment area as all likely positions of origin of the particles that enter the trap (Deuser et al., 1988), is advantageous to link changes in the surface ocean to those occurring in the water column. For this, we used a Lagrangian back-tracking model to determine the surface origin of particles arriving at 200 m at station HGIV, using the time-dependent velocity field of a high-resolution, eddy-resolving ocean-sea ice model (Wekerle et al., 2018). Daily particle trajectories were computed assuming a particle sinking velocity of 60 m d^{-1} (Wekerle et al., 2018; Fadeev et al., 2021b). The model was used to constrain the relative distribution of particle positions within the sediment trap catchment area from all trajectory calculations conducted daily for the time period 2002–2009. Particle distributions were binned into grid-cells to calculate weighted means. Grid cell size was determined from the available resolution of remote-sensing and model data products. Using these probability distributions for calculating weighted means provides a more realistic estimate than simply integrating over the areal extent of the catchment area. The spatial grid bins were used to calculate weighted means of sea ice coverage, sea surface temperature (SST) and chlorophyll *a*.

A sea ice concentration product was provided by CERSAT, the Satellite Data Processing and Distribution Center of the French Research Institute for Exploitation of the Sea (IFREMER), and is available on a 12.5 x 12.5 km grid (Ezraty et al., 2007). The ESA Ocean Color CCI Remote Sensing Reflectance (merged, bias-corrected) data are used to compute surface chlorophyll *a* concentration with a spatial resolution of 1 km^2 using the regional OC5ci chlorophyll *a* algorithms (Wekerle et al., 2018). The chlorophyll *a* data is interpolated to the sea ice grid size of 12.5 x 12.5 km. Model output from the Finite-Element Sea-ice Ocean Model (FESOM) was used to obtain salinity values and Mixed Layer Depth (MLD) (von Appen et al., 2021). Here we use a FESOM configuration adapted to the Fram Strait (Wekerle et al., 2017). Model products

were binned into 25 x 25 km grid cells and as for remote-sensing products, weighted means were calculated based on the relative proportion of particle trajectories in each grid cell. Mixed layer and stratified melt-water regimes have been previously defined in the Fram Strait and been shown to determine onset of biological production and export (von Appen et al., 2021). In the present study these regimes were defined in the catchment areas as follows: Unstratified (mixed layer depth >50m), mixed layer regime (ML) (mixed layer depth <50m and $(S_{100\text{m}} - S_{0\text{m}}) < 1$) and meltwater regime (MW) (mixed layer depth <50m and $(S_{100\text{m}} - S_{0\text{m}}) > 1$), where $S_{100\text{m}}$ and $S_{0\text{m}}$ are salinity values at 100 m and 0 m, respectively. The daily values of catchment area properties described above were integrated over the sediment trap opening period, considering a temporal lag of 4-days before the opening of the cup to reflect the impact of the changing environment that influenced the formation and export of the particles.

2.4 Distance to the sea ice edge

Distance of the sea ice edge (defined at 15% sea ice concentration) to the mooring site at the central HAUSGARTEN station (HGIV) was determined from remote sensing data. Satellite observations of daily sea ice were obtained from NSIDC/NOAA (<http://nsidc.org/data/nsidc-0051>). The product is based on the NASA Team algorithm and data mapped to a 25x25 km grid. Distances to the sea ice edge were averaged for the opening time of the sediment trap sample cups with a 4-day lag before the opening of the cup.

2.5 DNA extraction and Illumina amplicon sequencing

DNA analyses were done with splits of the original sediment trap sample (Table S3). Samples were sequentially filtered through 10, 3 and 0.2 μm polycarbonate membrane filters (Millipore, Schwalbach, Germany). DNA extraction was carried out using the NucleoSpin Plant Kit II (Machery-Nagel, Germany) following the manufacturer's protocol, and DNA concentrations were determined using the Quantus Fluorometer (Promega, United States). DNA extracts from the different fractions were pooled and amplified with a REPLI-g Mini Kit (Qiagen, Hilden, Germany) according to the manufacturer's protocol. Samples were stored at -20°C. The successful DNA isolation and amplification from mercury chloride-preserved sinking particle samples has been demonstrated previously (Metfies et al., 2017; Liu et al., 2020; Wietz et al., 2022). Storage times of up to 1 year did not have significant effects on the microbial community structure recovered from mercury-chloride fixed water samples (Wietz et al., 2022). To date, we are not aware of any studies that have tested longer storage times. Therefore, we cannot completely rule out that DNA degradation may have taken place over long storage times. This methodological challenge should be addressed in future studies.

2.6 16S and 18S rRNA amplicon sequencing

Library preparations were performed according to the standard instructions of the 16S Metagenomic Sequencing Library Preparation protocol (Illumina, Inc., San Diego, CA, United States). The hypervariable V3–V4 region of the bacterial 16S rRNA gene was amplified using bacterial primers S-D-Bact-0341-b-S-17 (5'-CCT ACG GGN GGC WGC AG-3') and S-D-Bact-0785-a-A-21 (5'-GAC TAC HVG GGT ATC TAA TCC-3' (Klindworth et al., 2013). For microbial eukaryotes, the hypervariable V4 region of the 18S rDNA gene was amplified with the primer set 528iF (5'-GCG GTA ATT CCA GCT CC-3') (Elwood et al., 1985) and 964iR (5'-AC TTT CGT TCT TGA TYR R-3' (Metfies et al., 2020). Sequencing was performed for 16S rRNA genes on the Illumina MiSeq platform in 2 × 300 bp paired-end runs (at CeBiTec, Bielefeld, Germany for bacteria, and at AWI, Bremerhaven, Germany for eukaryotes). Paired-end, primer-trimmed reads were deposited in the European Nucleotide Archive (ENA) at EMBL-EBI (Harrison et al., 2021) under accession numbers PRJEB43086 and PRJEB43576 for bacterial and eukaryotic data, respectively (<https://www.ebi.ac.uk/ena/browser/search>). Data were archived using the brokerage service of the German Federation for Biological Data (GFBio) (Diepenbroek et al., 2014), in compliance with the Minimum Information about any (x) Sequence (MIxS) standard (Yilmaz et al., 2011).

2.7 Bioinformatics and statistical analyses

Bacterial and eukaryotic libraries followed similar pipelines. Cutadapt was used to remove primer sequences from paired-end reads (Martin, 2011). The trimmed libraries were further processed using the package “DADA2” v. 1.14.1 (Callahan et al., 2016) in R v. 3.6.1 (<http://www.Rproject.org/>). DADA2 was used to differentiate amplicon sequence variants (ASVs) for both datasets, following the suggested workflow (<https://benjjneb.github.io/dada2/tutorial.html>). Briefly, after quality trimming and filtering of reads, dereplication was used to identify unique sequences and determine their abundance. The output of the dereplication and the error model were fed into the subsequent denoising step to resolve ASVs of up to one nucleotide difference using the quality score distribution in a probability model. Merging of the forward and reverse reads was performed with a minimum overlap by at least 10 bases. Chimeras and singletons were then filtered out from the dataset. The Silva reference database release 138 was used to assign taxonomy to the bacterial dataset (Quast et al., 2013), and PR v. 4.12.0 for the eukaryotic dataset (Guillou et al., 2013). ASVs unclassified at the highest taxonomic rank were removed, as were ASVs classified as *Mitochondria*, *Chloroplast* and *Craniata*. The final dataset consisted of 2,069,920 sequences; 672,992 18S rRNA sequences, and 1,396,928 16S rRNA sequences, from which 1,122 eukaryotic and 3,398 bacterial unique amplicon

sequence variants (ASVs) were identified. Rarefaction curves showed that the sequencing efforts applied were sufficient to describe the majority of the eukaryotic and bacterial diversity (Figure S1).

Statistical analyses and calculations in this study were performed using the R-package “phyloseq” v. 1.36.0 (McMurdie and Holmes, 2013). Alpha-diversity measurements and rarefaction curves were obtained using the R-packages “phyloseq” and “iNEXT” v. 2.0.20 (Hsieh et al., 2016). All beta-diversity parameters including dissimilarity matrices and hierarchical clustering based on Bray-Curtis dissimilarity, as well as statistical analyses and the centered log-ratio (clr) transformation of the ASV matrix were done using the “vegan” package v. 2.5-7 (Oksanen et al., 2013), and “tidyverse” v. 1.3.1 (Wickham et al., 2019). The ASVs fold-change between seasons were calculated using the R-package “DEseq2” v. 1.32.0 (Love et al., 2014).

Cross-domain co-occurrence network analyses between bacteria and eukaryotes were conducted separately for samples from different eukaryotic hierarchical clusters that were obtained from Bray-Curtis dissimilarity analyses. The network analyses were performed with the most abundant ASVs classified at the family level in each cluster (> 30%) using the “SpiecEasi” pipeline and the Meinshausen–Buhlmann neighborhood algorithm (R-package v.1.1.1) (Kurtz et al., 2015). To build the networks, the following parameters were used: lambda.min.ratio=1e-2, nlambda=20, rep.num=50. Constructed networks were visualized using the R-packages “igraph” v. 1.3.5 (Csardi and Nepusz, 2006), and “edgebundleR” v. 0.1.4 (Bostock et al., 2016).

We performed a Weighted gene correlation network analysis (WGCNA) using the R-package v. 1.70.3 (Langfelder and Horvath, 2008) to identify clusters of microbial ASVs by sorting ASVs into modules and correlating them with environmental variables (Guidi et al., 2016). Briefly, an ASV matrix was Hellinger-transformed and fed into a network topology analysis function, a signed network was used to preserve positively and negatively correlated nodes. Then, the adjacency matrix was used to create a topological overlap matrix (TOM). For this, adjacencies were calculated using the soft thresholding power of 14 for the eukaryotic data set and 8 for the bacterial data set. Module identification using dynamic tree cut was applied to the final selection of the modules. In total 18 modules were identified from the eukaryotic data set (ME_e) and 19 modules from the bacterial data set (ME_b). The first principal component of each module (i.e., eigenvalue) was Pearson-correlated with each environmental variable. The minimum size of the module eigenvalue was 35 for bacteria and 20 for eukaryotes to have a balanced number of ASVs per module. Variables were: SST, chlorophyll *a* and sea ice concentration (%) from the backward Lagrangian particle tracking model, distance to the sea ice edge, daylight hours, biogenic fluxes (POC, Si and CaCO₃) and total swimmer flux measured from sediment trap samples (Ramondenc et al., 2022) as a representation of zooplankton occurrence in the water column, and modelled water regime proportions (unstratified, ML, MW regimes as proportions).

3 Results

3.1 Oceanographic setting: general trends of sea ice concentration, chlorophyll *a* concentration, temperature and stratification regimes from 2000 to 2012

The location investigated here in eastern Fram Strait ($\sim 79.01^\circ\text{N}$, $\sim 4.20^\circ\text{E}$, water depth ~ 2500 m) is often influenced by the marginal ice zone (Soltwedel et al., 2016) (Figure 1). At the time of spring and summer high particle flux (HPF) events, sea ice concentration remained on average below 2% (range: 0 – 17%). With the exception of one spring sampling event with a sea ice concentration of 17%, sea ice concentration was higher in summer (1%) compared to spring (0.8%) (Table S1 and Figure S2). Sea ice concentration displayed great interannual variability, i.e. was lower during the WWA period (0 – 3%) and increased after 2007 (0.3 – 17%). Distances to the sea ice edge varied from 4 km to 116 km. Coinciding with higher sea ice concentration in the catchment area, distances to the sea ice edge were shorter (average 38 km) towards the end and after the WWA (2007 – 2011), while they were generally higher during the summer events (average 56 km). SST varied according to seasonality, with warmer values (2 – 4.8°C) in the summer, and colder (0.6 – 1.5°C) during the spring events. Temperatures above 1.4°C were recorded during the spring period at the time of the WWA. Satellite-based chlorophyll *a* values ranged from 0 – 0.56 mg m³ throughout the 12 years of observation. The HPF occurred during periods with between 8 h and 24 h (average 20 h) of daylight; only two spring samples were below 15 h of daylight in 2001 and 2005 (i.e. 8 and 10 h of daylight, respectively).

The substantial interannual differences in sea ice presence in the catchment area were also reflected in different water stratification regimes that were modelled for the region. The water column in the pre-WWA and post-WWA years was mostly characterized by the

MW regime (average: 73% and 51% respectively) (Table S1 and Figure S3). In contrast, the period of the WWA was characterized by weaker stratification and rather qualified as a ML regime. Unstratified waters were present in our data set early in spring (on average 41% in spring and <1% in summer events). Overall, 2000, 2005 and 2012 shared a higher proportion of unstratified water, but otherwise a combination of ML and MW regimes dominated spring from 2000 to 2012 (Figure S4). Towards the Arctic summer, HPF shared a higher proportion of MW (66%) over ML (33%).

3.2 Export fluxes during HPF events

Usually two HPF events were observed per year, in spring and summer (Figure 2). Throughout the time-series, HPF events provided 1.6% to 40.7% (average 14.5%) of the total POC flux per sampling period (total time of collection by sediment trap) (Table 1). Summer events were on average higher (average 26.57 mg m⁻² d⁻¹, range: 4.75 – 49.37) than spring events (average 16.36 mg m⁻² d⁻¹, range: 7.61 – 24.19), but differences were not significant (ANOVA $p > 0.05$). Export flux (mg C m⁻² d⁻¹) during HPF events did not show significant differences between the WWA categories (pre-WWA, WWA and post-WWA; ANOVA $p > 0.05$), due to the high interannual variation, and the few time-points available for the WWA. However, during the WWA the HPF was substantially lower (average 13.55 mg m⁻² d⁻¹, range: 4.75 – 23.95) compared to pre-WWA (average 25.56 mg m⁻² d⁻¹, range: 9.13 – 49.37) and post-WWA values (average 26.61 mg m⁻² d⁻¹, range: 10.02 – 46.73).

Trends in PON flux generally agreed with POC flux during HPF events (Figure S5). The summer-PON fluxes were higher (average 3.56 mg m⁻² d⁻¹, 0.54 – 7.10) compared to spring-PON fluxes (average 1.90 mg m⁻² d⁻¹, range: 0.70 – 3.77), but not significantly (ANOVA $p > 0.05$). Like POC fluxes, PON fluxes did not show significant differences between the WWA categories (ANOVA $p >$

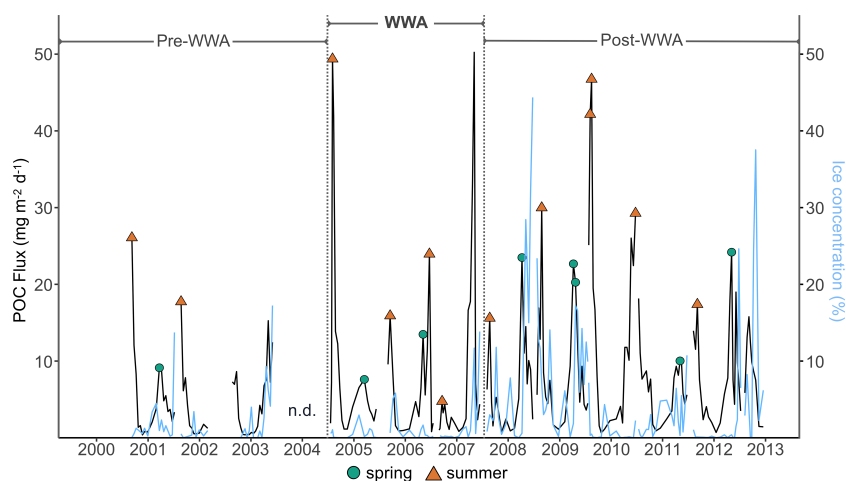


FIGURE 2

POC flux (mg m⁻² d⁻¹) (black), and ice concentration (%) (blue) in the catchment area of the sediment trap at the mooring location of the central station (HGIV) for the period from 2000 to 2012. The peak POC values selected for this study are noted by green circles for highest POC export fluxes (HPF) in spring and orange triangles for summer HPF events. n.d.; Data not determined.

0.05). During HPF events, C:N ratios were mostly similar throughout the time series, and close to Redfield with on average 8.8 in spring and 10.1 in summer (Table S1). The highest ratios (> 12) were observed in samples from August 2001, August 2009, and from March 2005; lowest ratios occurred in May 2012, April 2008, August 2008 and in April 2009.

Si and CaCO₃ fluxes displayed high interannual variability. Peaks in Si fluxes were mostly observed in late summer and in autumn, and CaCO₃ fluxes were higher in winter and autumn, thus the spring and summer HPF were not coupled to the highest Si and CaCO₃ flux events (Bauerfeind et al., 2014) (Figure S5). Si fluxes measured during summer HPF events corresponded to 38% of the

total Si flux per sampling period, and in spring 9.4% of the total Si flux per sampling period (Table 1). Si fluxes measured during summer HPF were significantly higher compared to spring HPF events (Kruskal-Wallis test; Chi square=7.4, df=1, p-value<0.01). Si: POC ratios were on average 0.02 in spring, and 0.13 in summer (Table S1). Si fluxes were much higher in early years of the investigated period (average 18.35 mg m⁻²d⁻¹, range: 0.32 – 37.30), compared to the period of the WWA (2.33 mg m⁻² d⁻¹, range: 0.29 – 8.51); Si fluxes slightly increased again after that, but remained low for the post-WWA period (2.37 mg m⁻² d⁻¹, range: 0.36 –10.49). CaCO₃ fluxes measured during summer HPF events corresponded to 26% of the total CaCO₃ fluxes per sampling period

TABLE 1 Total biogenic flux per sampling period and the contribution of the highest POC export fluxes (HPF) to total flux.

Sediment trap ID	Sampling period	Total number of days (n)	Total POC flux per sampling period (g m ⁻²)	Contribution of HPF (%) to total POC flux during the sampling period	Total Si flux per sampling period (g m ⁻²)	Contribution of Si flux (%) to total Si flux during the sampling period	Total CaCO ₃ flux per sampling period (g m ⁻²)	Contribution of CaCO ₃ flux (%) to total CaCO ₃ flux during the sampling period
FEVI1	2000/2001	317	1.58	24.8	1.43	63.7	1.02	24.5
				8.7		0.1		2.4
FEVI2	2001/2002	212	0.74	40.7	0.1	55	0.92	74.1
FEVI3	2002/2003	300	1.33	9.7*	1.18	6.8	0.94	13.9
				17.2*		52.4		25.5
FEVI7	2004/2005	335	2.39	14.5	1.55	71.1	2.00	32.5
				17.6*		25.4		35.6
				9.9		0.1		7.6
FEVI10	2005/2006	330	1.87	17	0.11	23.7	0.57	22.3
				10.8		6.8		9.2
				19.2		11.6		24.4
FEVI13	2006/2007	298	2.12	1.6	0.12	0.2	0.72	1.1
				23.6*		20.7		18.9
				23.7*		14.5		26
FEVI16	2007/2008	344	1.97	13.4	0.20	58.6	0.90	15.5
				17.9		3.1		16.7
FEVI18	2008/2009	370	2.78	11.9	0.27	58.4	1.59	17.3
				12.3		1.1		9.7
				10.9		2.3		11.5
FEVI20	2009/2010	345	3.82	11	0.23	2.1	1.70	9.2
				12.2		55.5		33.7
				11.5		1		6.1
FEVI22	2010/2011	355	1.97	5.1	0.05	7.3	1.02	3.9
FEVI24	2011/2012	349	2.37	7.4	0.21	35.9	2.43	28.8
				10.2		0.9		6.5

Total values per sample were calculated based on the number of days the sampling cup was open during deployment. Note that the sampling period for 2000 started in 2000-08-31 and that the electronic failure of sediment traps during the 2003-2004 operational year and from mid-March through July 2002 prevented the collection of samples. Samples not included in the study are marked with an asterisk (*) and are included here for overview.

compared to 13% in spring (Table 1). CaCO₃ fluxes were significantly higher in the post-WWA period (Post-hoc Wilcoxon, *p*-adjust < 0.01).

3.3 Microbial composition of sinking particles during HPF events

3.3.1 Eukaryotic community

The eukaryotic microbiome of sinking particles during HPF events was dominated by diatoms (*Bacillariophyta*), dinoflagellates (*Syndiniales*), and radiolarians (*Acantharea*), together they comprised 59% of the eukaryotic sequences. *Bacillariophyta* were mainly comprised of the common Arctic diatom genera *Chaetoceros*, *Thalassiosira* and *Melosira*. *Syndiniales* were dominated by members of the orders *Dino-Group-I*, and *Dino-Group-II* that represented 20% of the eukaryotic ASVs. *Acantharea* were strongly dominated by ASVs of the order *Chaunacanthida*. Metazoans comprised 5% of the total ASVs. The division *Metazoa* was strongly dominated by sequences of copepod taxa, mainly *Calanus*, *Neocalanus* and *Metridia*.

A transition in the dominance of diatom ASVs was linked to the WWA. From 2004 to 2006 *Thalassiosira* clr-transformed ASV

counts increased from 3 to 11 (peaked in 2005) and dominated diatom sequences only during this period (Figure 3). *Thalassiosira* was also the most dominant diatom in early samples with low light (8 – 11 h) in March 2001 and 2005 (0.6 and 11 clr-transformed ASV counts, respectively; Figure 3). Towards the peak of the WWA in 2006 all diatom sequences decreased substantially and only *Melosira* showed a peak in September 2006 with 17 clr-transformed ASVs. Moreover, in 2006 the fungi classes *Basidiomycota* and *Chytridiomycota* significantly increased, concomitant with the sharp decrease of diatom sequences (Figure S6).

In a hierarchical clustering based on Bray-Curtis dissimilarity (Figure 4A), the eukaryotic community clustered into 3 main groups without chronological order; 1e, 2e and 3e. The first cluster 1e grouped samples from the summer events and contained a high proportion of heterotrophic and mixotrophic eukaryotes of the classes *Acantharea*, *Dinophyceae* and *Syndiniales*. The second cluster 2e comprised mainly samples from the WWA period (Table S1 and Figure 4A), and was characterized by an increased proportion of heterotrophic pico- and nano-plankton taxa such as MAST-9, MAST-1, and other protists like the heterotrophic *Filosa-Thecofilosea* and *Telonemia*. ASVs affiliated with diatoms decreased compared to previous years and the dominant *Chaetoceros* was absent in the

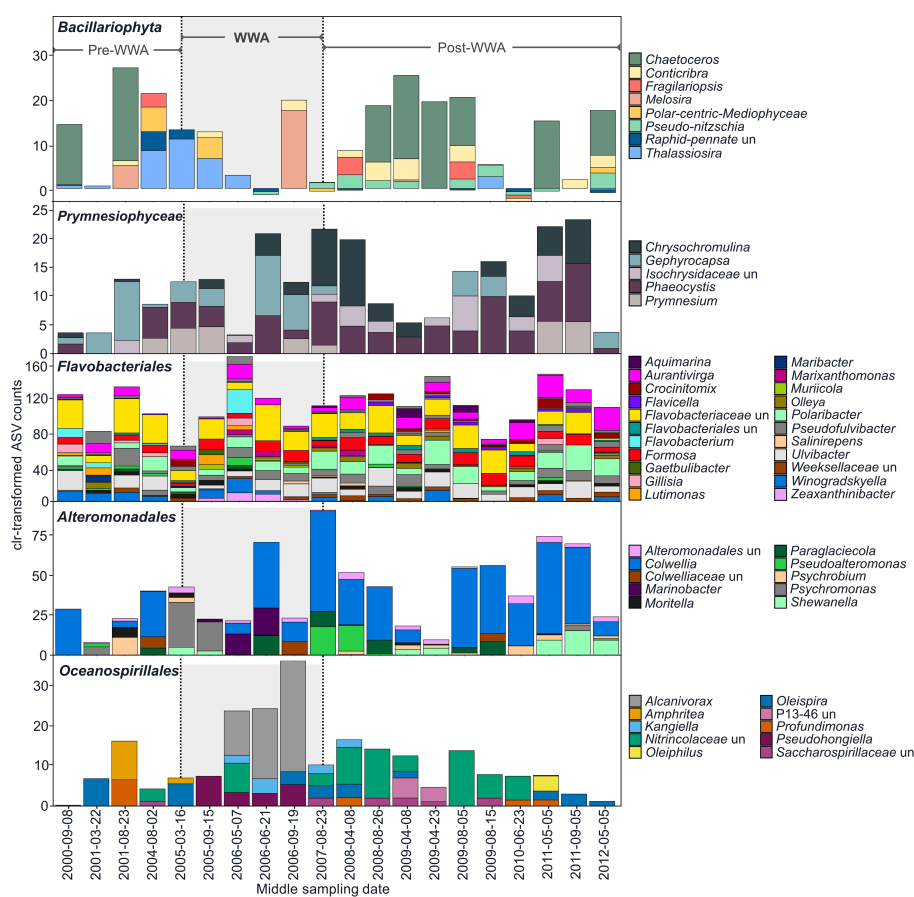
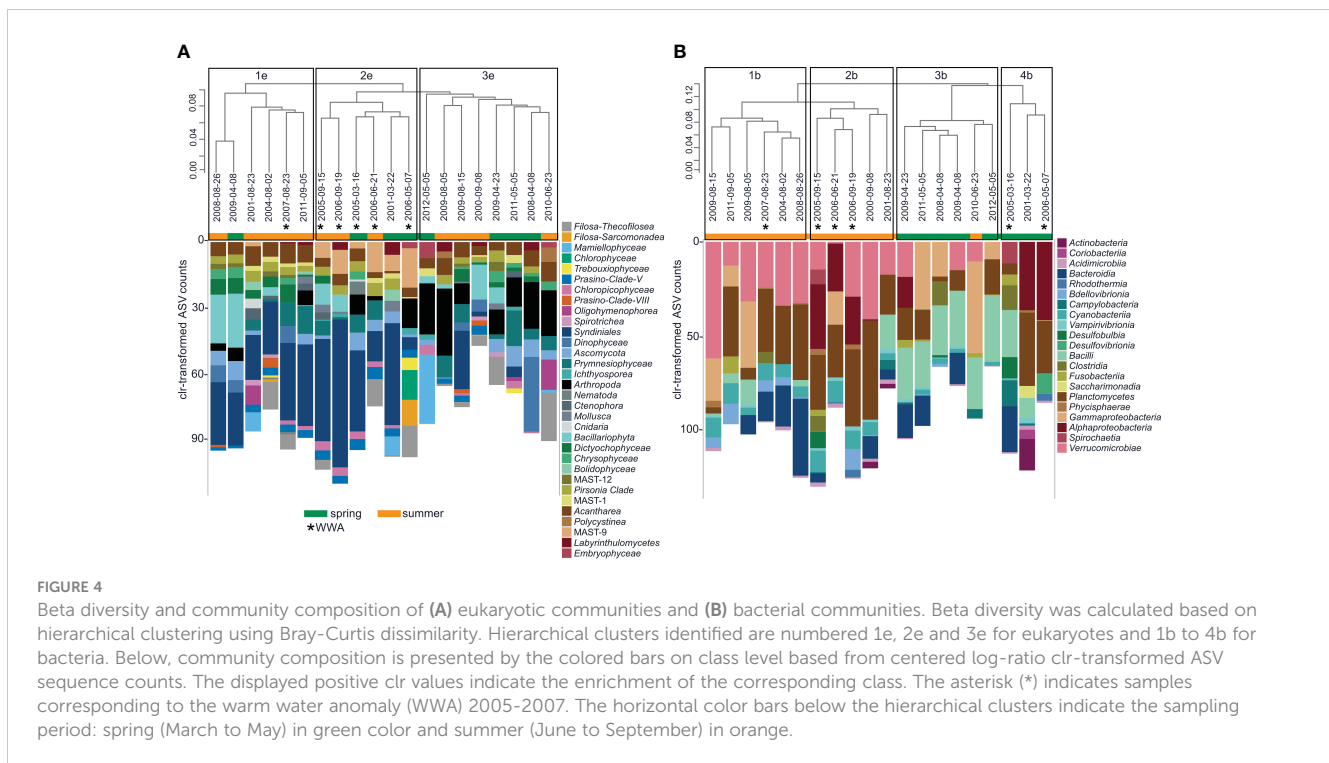


FIGURE 3
Main changes in selected groups of eukaryotes (diatoms and flagellates) and main bacterial orders based on centered log-ratio clr-transformed ASV counts. Dates correspond to the middle date of the sampling period. The light gray area in the background panels behind the bars indicates the WWA period from 2005 to 2007. Un, unclassified.



second cluster (0 clr-transformed ASVs in WWA samples, compared to 14 – 21 in pre-WWA and 10 – 20 post-WWA samples; Figure 3). Moreover, the second cluster was also characterized by an increase of the only coccolithophore identified on genus level *Gephyrocapsa* and the increase of flagellate ASVs assigned to *Phaeocystis* and *Prymnesium* towards the end of the WWA period (Figure 3). The third cluster 3e corresponded to samples that were all from the post-WWA period (Figure 4A). Samples from the third cluster showed a higher representation of autotrophic groups such as *Prymnesiophyceae* (*Haptophyta*), including the flagellates *Phaeocystis*, *Chrysochromulina* and *Prymnesium* and a few members of the *Chlorophyta*, mainly *Mamiellophyceae*. These samples were also marked by an increase of zooplankton taxa, especially copepods (*Calanus*), which comprised a significant proportion of the community, as well as fungi sequences affiliated with *Ascomycota*. Diatom sequences in the third cluster were mainly represented by *Chaetoceros* (Figure 3).

3.3.2 Bacterial community

Bacterial communities were strongly dominated by typical phytoplankton-associated bacteria, mainly the classes *Gammaproteobacteria*, *Bacteroidia*, *Alphaproteobacteria* and *Verrucomicrobiae* (Figure 4B). Thirty percent of the bacterial ASVs were classified as *Gammaproteobacteria* mainly of the orders *Cellvibrionales* and *Alteromonadales*. *Bacteroidales* was dominated by the diatom-associated order *Flavobacteriales*, which represented 13% of the bacterial ASVs. Zooplankton-associated taxa of the order *Entomoplasmatales* (class *Bacilli*), the majority assigned to *Candidatus Hepatoplasma*, comprised 14% of the total community and strongly dominated samples of the spring events and only after the WWA period.

The bacterial community clustered into 4 groups based on beta diversity assessment (Figure 4B, clusters 1b to 4b). In the first and second cluster 1b and 2b, the majority of the samples consisted of summer events and contained a higher representation of *Verrucomicrobiae* and *Planctomycetes*, whereas the third and fourth cluster grouped samples of the spring events. The third cluster 3b was characterized by a strong presence of *Gammaproteobacteria* and *Bacilli* (Figure 4B). Bacterial communities of the WWA clustered in two branches, unlike the eukaryotic community, i.e. the second and fourth cluster, except for one sample from August 2007. The fourth cluster 4b did not contain *Verrucomicrobiae* sequences, and unlike other spring samples the fourth cluster was also characterized by a notable decrease in the number of *Bacilli* sequences (Figure 4B).

3.4 Seasonality (early vs. late export events)

Microbial community composition showed a strong seasonal separation, particularly in the bacterial clusters (Figure 4B). To further explore the seasonality of the microbial composition of the sinking particles, we grouped samples into spring and summer (Table S1) and identified the respective core communities. We defined core taxonomic groups as those present in all samples of one season, and with sequence abundances >0.5% of the eukaryotic seasonal data set, and >1.5% for the bacterial data (Tables 2, 3). The great majority of the core ASVs belonged to the most abundant orders in the dataset. We did not identify unique taxa for spring and summer. But the majority of the most abundant core ASVs showed changes in the proportions between seasons. In total, 7 eukaryotic and 14 bacterial core ASVs were found to be present across the datasets.

3.4.1 Seasonality of eukaryotic communities

In spring events, the core eukaryotic ASVs comprised 44% of the total eukaryotic community, and in the summer events the core ASVs were 42% of the total community (Table 2 and Figure S7A). The spring core community was dominated by an ASV of the order *Dino-Group-I* (8.5%) with a similar sequence abundance in the summer (7.8%), followed by the copepod *Calanus* (6%) and an unclassified ASV of the radiolarian class *Chaunacanthida* (4%), consistent with the early stages of the phytoplankton bloom. Higher abundances of *Chaunacanthida* and *Chaetoceros* were observed in summer events. *Chaunacanthida* comprised 27% of all summer sequences. *Chaetoceros* made up 4% of the community in spring, and 13% in the summer. The flagellate *Phaeocystis* and the chlorophyte *Micromonas* were also part of the summer core community.

3.4.2 Seasonality of bacterial communities

Based on beta diversity assessments presented in section 3.3.2, bacterial communities showed a stronger separation between spring and summer events compared to eukaryotic communities. The proportion of the bacterial microbiome represented by core bacterial ASVs was substantially higher in the summer events (40%) than in the spring events (25%). The spring events were dominated by two *Candidatus* Hepatoplasma ASVs and one *Mycoplasma* ASV, which together made up 38% of the spring community (Table 3). *Candidatus* Hepatoplasma ASVs were also part of the core community in summer events (7%), highlighting the prominence of this taxonomic group in the sinking particles.

Overall, *Flavobacteriales*, *Gammaproteobacteria* and *Verrucomicrobiales* ASVs were present both in spring and summer core communities, but made up higher proportions in summer (Table 3). *Flavobacteriales* core ASVs comprised 11% of spring communities and 21% of summer communities; the latter were dominated by *Formosa* (6.3%). *Luteolibacter* (*Verrucomicrobiales*) and ASVs of the *Gammaproteobacteria* clade OM60(NOR5), together comprised 13% of all summer sequences. Core ASVs of *Formosa*, *Luteolibacter* and an ASV of the OM60(NOR5) clade showed a twofold increase in summer events (Figure S7B). Moreover, summer events had a higher number of ASVs typically associated with phytoplankton, which included *Flavobacteriales*, *Verrucomicrobiales* and *Cellvibrionales* ASVs (Figure 4B and Table 3).

3.5 Microbial connectivity in sinking particles

Although bacterial communities did not cluster fully in line with eukaryotic community clusters, overall changes in bacterial community structure were significantly correlated with changes in the eukaryotic community (Mantel test $r=0.38$, $p=0.001$). Eukaryotes are the main particle formers, to which most bacteria will be associated either as part of their natural microbiome or as a result of attachment and colonization. To address potential associations between bacteria and eukaryotes in the sinking particles, co-occurrence networks were constructed from families of the three identified eukaryotic clusters (cluster 1e, 2e and 3e

Figure 4A). In all three networks, the proportion of positive associations was higher (56% – 58%) than negative ones (42% – 44%), with little variation between the three networks. Overall, the networks of the first, second and third cluster consisted of 531, 487, and 420 nodes of bacterial and eukaryotic ASVs, respectively.

Based on co-occurrence, the highest number of potential associations between bacteria and eukaryotes in all three networks involved families of the bacterial orders *Alphaproteobacteria* and *Gammaproteobacteria* with alveolate families of the *Syndiniales* and *Dinophyceae*, and pico- and nano-plankton affiliated with marine stramenopiles (MAST) (Figure 4A). In the network of the first cluster, co-occurrences between *Syndiniales* and other eukaryotes like *Haptophyta* and *Stramenopiles* were substantial compared with the second and third cluster networks. *Syndiniales* comprised 7% of the sequences in the network. Of the *Syndiniales*, families of *Dino-Group-II* showed the highest number of potential associations with bacterial families of *Gammaproteobacteria* and *Alphaproteobacteria* (Figure S8). MAST families co-occurred with other *Syndiniales*, and *Haptophyta*. Families of diatoms, which made up 8% of the community of the first network, co-occurred diversely with *Fungi*, *Syndiniales*, *Chlorophyta* and few bacterial families including *Flavobacteriales*, which contributed 14% of the sequences in the first network.

In the second cluster, co-occurrences between eukaryotic families and proteobacterial families were numerous, mainly including families that increased during the WWA (Figure S9) although families of the *Flavobacteriales* comprised the majority of bacterial sequences in the second network (16% of the network community). For instance, a *Telonemia-Group-2* family co-occurred with 4 *Gammaproteobacteria* and *Alphaproteobacteria* families. Similarly, *Sandonidae* a family of the *Filosa-Sarcomonadea* co-occurred with 4 families of the *Gammaproteobacteria* and *Saccharimonadales*. Families of the orders MAST-9, MAST-1, and MAST-12 co-occurred with 22 *Proteobacteria* families of the *Gammaproteobacteria* and *Alphaproteobacteria* which increased during the WWA and included families of the *Oceanospirillales* (5% of the network community), *Alteromonadales* (6% of the network community) (e.g. *Marinobacteraceae*), and *Micavibrionales* (<1% of the network community). The coccolithophore family *Noelaerhabdaceae* that includes *Gephyrocapsa* co-occurred with 5 bacterial families, and the flagellate families *Phaeocystaceae*, *Prymnesiaceae* and *Chrysochromulinaceae* showed co-occurrence with 15 bacterial families. The diatom families *Polar-centric-Mediophyceae* and *Radial-centric-basal-Coscinodiscophyceae* were potentially associated with 8 bacterial families of the *Flavobacteriaceae*, *Oceanospirillales*, *Desulfocapsaceae*, *NB1-j* and *Micavibrionales*. Co-occurrences between *Proteobacteria* families were stronger and more numerous in the second cluster compared to the other clusters including alphaproteobacterial families (e.g. *Rhizobiales*, *Rhodospirillales*, *Bacteroidales*, *Flavobacteriales*) and gammaproteobacterial families (e.g. *Alteromonadales*, *Cellvibrionales*, *Cellvibrionales*).

In the third cluster, only 4 potential associations between families of flagellates and bacterial families of *Gammaproteobacteria* and *Alphaproteobacteria* were observed (Figure S10). Families of the orders MAST-9, MAST-1 were associated with 13 bacterial families. Families of MAST affiliation co-occurred with numerous

TABLE 2 Most abundant core sequences in the 18S rRNA assemblages in sinking particles in spring (March to May) and summer (June to September) from 2000 to 2012.

ASV	Absolute sequence abundance in the season	% sequence abundance in the season	Absolute sequence abundance in data set	% sequence abundance in data set	Eukaryotic taxonomic classification				
					Supergroup & Division	Class	Order	Family	Genus
Spring events									
sq4	14063	8.5	53457	7.9	<i>Alveolata; Dinoflagellata</i>	<i>Syndiniales</i>	<i>Dino-Group-I</i>	<i>Dino-Group-I-Clade-1</i>	<i>Dino-Group-I-Clade-1 un</i>
sq8	9932	6	12983	1.9	<i>Opisthokonta; Metazoa</i>	<i>Arthropoda</i>	<i>Crustacea</i>	<i>Maxillopoda</i>	<i>Calanus</i>
sq1	6854	4.1	144013	21.4	<i>Rhizaria; Radiolaria</i>	<i>Acantharea</i>	<i>Chaunacanthida</i>	<i>Chaunacanthida un</i>	<i>Chaunacanthida un</i>
sq2	6076	3.7	72884	10.8	<i>Stramenopiles; Ochrophyta</i>	<i>Bacillariophyta</i>	<i>Bacillariophyta un</i>	<i>Polar-centric-Mediophyceae</i>	<i>Chaetoceros</i>
sq9	5579	3.4	10333	1.5	<i>Archaeplastida; Chlorophyta</i>	<i>Mamiellophyceae</i>	<i>Mamiellales</i>	<i>Mamiellaceae</i>	<i>Micromonas</i>
sq21	2645	1.6	3791	0.6	<i>Opisthokonta; Fungi</i>	<i>Ascomycota</i>	<i>Pezizomycotina</i>	<i>Sordariomycetes</i>	<i>Simplicillium</i>
Summer events									
sq1	137159	27	144013	21.4	<i>Rhizaria; Radiolaria</i>	<i>Acantharea</i>	<i>Chaunacanthida</i>	<i>Chaunacanthida un</i>	<i>Chaunacanthida un</i>
sq2	66808	13.2	72884	10.8	<i>Stramenopiles; Ochrophyta</i>	<i>Bacillariophyta</i>	<i>Bacillariophyta un</i>	<i>Polar-centric-Mediophyceae</i>	<i>Chaetoceros</i>
sq4	39394	7.8	53457	7.9	<i>Alveolata; Dinoflagellata</i>	<i>Syndiniales</i>	<i>Dino-Group-I</i>	<i>Dino-Group-I-Clade-1</i>	<i>Dino-Group-I-Clade-1 un</i>
sq9	4754	0.9	10333	1.5	<i>Archaeplastida; Chlorophyta</i>	<i>Mamiellophyceae</i>	<i>Mamiellales</i>	<i>Mamiellaceae</i>	<i>Micromonas</i>
sq28	2402	0.5	3442	0.5	<i>Hacrobia; Haptophyta</i>	<i>Prymnesiophyceae</i>	<i>Phaeocystales</i>	<i>Phaeocystaceae</i>	<i>Phaeocystis</i>

Core community members were defined as those present in all samples for each corresponding season (spring or summer). Total number of eukaryotic sequences in the spring = 165648, and in the summer = 507344. Only ASVs with more than 0.5% sequence abundance in the eukaryotic data were included in this table. Un, unclassified.

TABLE 3 Most abundant core sequences in 16S rRNA assemblages in sinking particles in spring (March to May) and summer (June to September) from 2000 to 2012.

ASV	Absolute sequence abundance in the season	% sequence abundance in the season	Absolute sequence abundance in data set	% sequence abundance in data set	Bacterial taxonomic classification				
					Phylum	Class	Order	Family	Genus
Spring events									
sq1	126890	21.6	151327	10.8	<i>Firmicutes</i>	<i>Bacilli</i>	<i>Entomoplasmatales</i>	<i>Entomoplasmatales Incertae Sedis</i>	<i>Candidatus Hepatoplasma</i>
sq2	70607	12	105311	7.5	<i>Firmicutes</i>	<i>Bacilli</i>	<i>Entomoplasmatales</i>	<i>Entomoplasmatales Incertae Sedis</i>	<i>Candidatus Hepatoplasma</i>
sq9	26406	4.5	28445	2	<i>Firmicutes</i>	<i>Bacilli</i>	<i>Mycoplasmatales</i>	<i>Mycoplasmataceae</i>	<i>Mycoplasma</i>
sq8	16901	2.9	30471	2.2	<i>Bacteroidota</i>	<i>Bacteroidia</i>	<i>Flavobacteriales</i>	<i>Flavobacteriaceae</i>	<i>Polaribacter</i>
sq14	14909	2.5	21483	1.5	<i>Bacteroidota</i>	<i>Bacteroidia</i>	<i>Flavobacteriales</i>	<i>Flavobacteriaceae</i>	<i>Aurantivirga</i>
Summer events									
sq4	50727	6.3	52368	3.8	<i>Bacteroidota</i>	<i>Bacteroidia</i>	<i>Flavobacteriales</i>	<i>Flavobacteriaceae</i>	<i>Formosa</i>
sq3	48319	6	55070	3.9	<i>Verrucomicrobiota</i>	<i>Verrucomicrobiae</i>	<i>Verrucomicrobiales</i>	<i>Rubritaleaceae</i>	<i>Luteolibacter</i>
sq2	34704	4.3	105311	7.5	<i>Firmicutes</i>	<i>Bacilli</i>	<i>Entomoplasmatales</i>	<i>Entomoplasmatales Incertae Sedis</i>	<i>Candidatus Hepatoplasma</i>
sq5	32526	4	34463	2.5	<i>Proteobacteria</i>	<i>Gammaproteobacteria</i>	<i>Cellvibrionales</i>	<i>Halieaceae</i>	OM60(NOR5) clade
sq1	24437	3	151327	10.8	<i>Firmicutes</i>	<i>Bacilli</i>	<i>Entomoplasmatales</i>	<i>Entomoplasmatales Incertae Sedis</i>	<i>Candidatus Hepatoplasma</i>
sq6	23202	2.9	31638	2.3	<i>Bacteroidota</i>	<i>Bacteroidia</i>	<i>Flavobacteriales</i>	<i>Flavobacteriaceae</i>	<i>Polaribacter</i>
sq13	20799	2.6	22131	1.6	<i>Verrucomicrobiota</i>	<i>Verrucomicrobiae</i>	<i>Verrucomicrobiales</i>	<i>Rubritaleaceae</i>	<i>Luteolibacter</i>

Core community members were defined as those present in all samples for each corresponding season (spring or summer). Total number of bacterial sequences in the spring = 587590, and in the summer = 809338. Only ASVs with more than 2.5% in the bacterial data set were included in this table.

other eukaryotes, a feature also observed in the constructed network of the first cluster, but not observed in the network of the second cluster. Notably, 12% of the sequences in this network were assigned to the copepod class *Arthropoda*. Six bacterial families of the *Gammaproteobacteria* (15% of the network community), including *Porticococcaceae* and *Burkholderiaceae* were associated with the copepod family *Maxillopoda* and a *Metazoan* family. Moreover, the *Chaetoceros* family *Polar-centric-Mediophyceae* which comprised 7% of the community in the third network, potentially associated with the bacterial families *Pirellulaceae*, *Burkholderiaceae*, *Nitrincolaceae* and *Caulobacteraceae*.

3.6 Relationship between environmental parameters and microbial composition of sinking particles

The changes observed in the microbial composition of the sinking particles suggest that the different communities reflected oceanographic variations in the eastern Fram Strait related to sea ice, meltwater and daylight (Figures 3, 4). To investigate decadal changes in the particle-associated microbial community associated with changing environmental conditions marked by the WWA, we performed a WGCNA, a method applied to study microbial communities and correlations with environmental traits (e.g. Duran-Pinedo et al., 2011; Guidi et al., 2016; Wilson et al., 2018).

In addition, we identified the main ASVs in each module as candidate microbial indicators (Figure 5).

3.6.1 Eukaryotic community

Eight eukaryotic modules ME_e , from 18 identified in total, correlated with environmental variables (Figure 5A). Two modules ME_e 2 and ME_e 5 correlated with the changing ice concentration and distance to the ice edge. ME_e 2 displayed a strong positive correlation with ice concentration (Pearson's correlation; $r=0.94$, p -value<0.01). ME_e 2 was comprised mostly of ASVs of *Dino-Group-I* (18%), the dinoflagellate *Heterocapsa* (15%), and ASVs of diatoms mainly *Chaetoceros* (8%), coinciding with the higher concentration of ice before and after the WWA (Figure 5A). ME_e 5 correlated positively with distance to the sea ice, SST, $CaCO_3$ flux and swimmer flux (Pearson's correlation; $r>0.51$, p -value<0.02). ME_e 5 was dominated mainly by summer taxa (Table 2), ASVs of the order *Dino-Group-II* (23%), and small flagellates including *Dictyochophyceae* (9%) and *Prymnesiales* assigned to *Chrysochromulina* (8%).

ME_e 3 and ME_e 8 correlated positively with the unstratified water regime characteristic of the spring (Pearson's correlation; $r>0.4$, p -value<0.05) (Figure S4A). ME_e 3 had the largest proportion of mixotrophs and heterotrophs, particularly dinoflagellate ASVs affiliated with *Gymnodinium* (15%), and the orders *Dino-Group-II* (11%), and *Strombidiida* (7%) (Figure 5A). ME_e 8 correlated negatively with daylight and the MW regime. ME_e 8 was

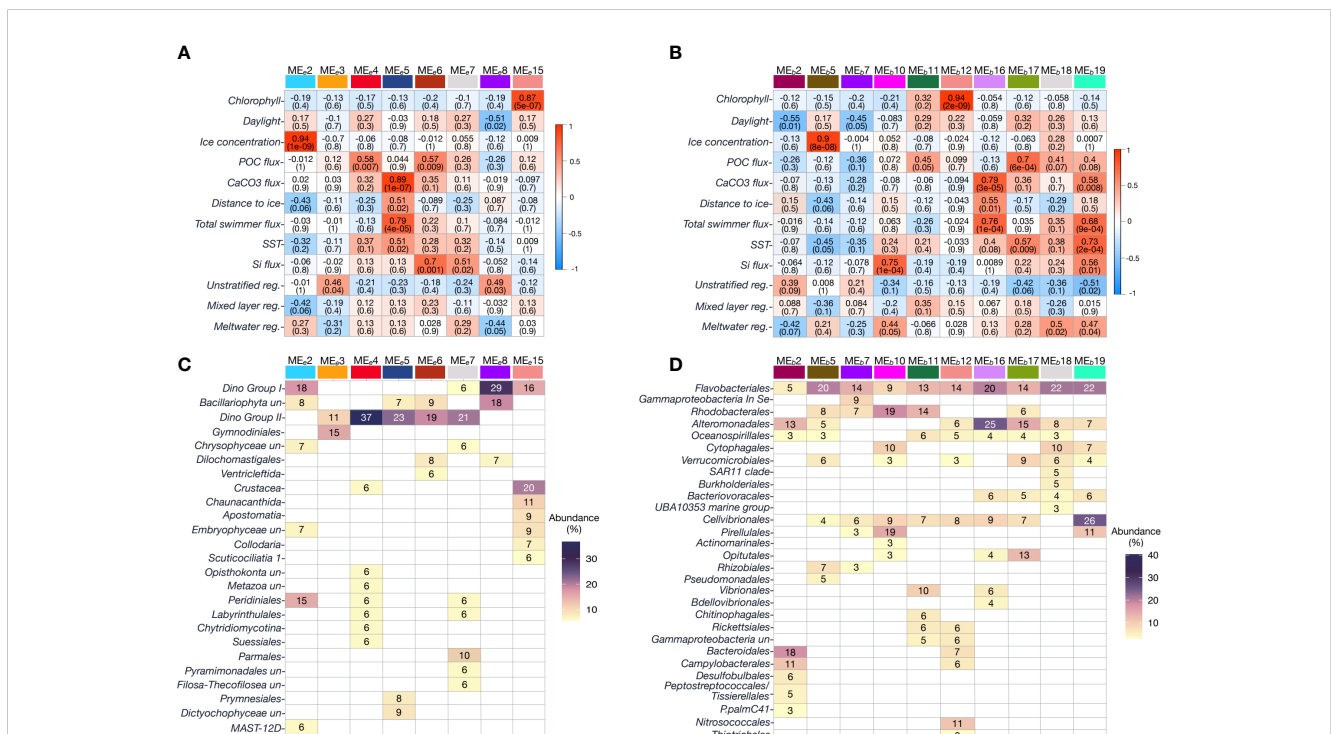


FIGURE 5

Weighted gene correlation network analysis WGCNA on eukaryotic communities (A, C) and bacterial communities (B, D). Top heatmaps (A, B) indicate Pearson's correlation coefficient between environmental parameters and microbial module Eigengenes (ME_e for eukaryotes and ME_b for bacteria). Only modules with significant correlations (p -value<0.05) for at least one correlation pair were included; p -values are indicated in parentheses. Modules are color-coded for easier distinction. Lower panels (C, D) represent the phylogenetic affiliation and relative abundance of different ASVs in each module grouped at order level. Only ASVs with abundances higher than 5% were included in the plot. Un, unclassified. In Se, Incertae Sedis.

comprised mostly of ASVs of *Dino-Group-I* (29%) and *Thalassiosira* (18%). With the exception of one sample in summer 2009, sequences of *Thalassiosira* were only detected in 2004, 2005 and 2006 towards the WWA, which was also characterized by a smaller proportion of the MW regime (Figure S4B).

3.6.2 Bacterial community

Ten of 19 bacterial modules ME_b correlated significantly with environmental variables (Figure 5B). The order *Flavobacteriales* dominated in the majority of the modules, followed by *Alteromonadales* and *Rhodobacterales*.

ME_{b5} was the only module that correlated strongly and positively with ice concentration (Pearson's correlation; $r=0.9$, p -value <0.01), and negatively with SST (Pearson's correlation; $r=-0.45$, p -value $=0.05$). *Flavobacteriales* dominated 20% of the ME_{b5} including *Ulvibacter*, *Polaribacter*, *Winogradskyella* and *Maribacter* followed by unassigned ASVs of the *Rhodobacteraceae* family that increased only in pre-WWA (8%) (Figure 5B), and *Methylobacterium-Methylorubrum* (*Rhizobiales*) a species only detected in post-WWA samples.

ME_{b2} and ME_{b7} showed negative correlations with daylight (Pearson's correlation; $r<-0.45$, p -value <0.01). ME_{b2} was the only module with a high proportion of members of the *Marinifilaceae* family (18%) (*Bacteroidales*) which were only present in samples with less than 11 h of daylight in March of 2005 and 2001, followed by *Psychromonas* and *Moritella* (*Alteromonadales*) also identified in 2001 and 2005 (Figure 3). ME_{b7} contained a large number of *Flavobacteriaceae* (14%) (Figure 5B).

ME_{b19} correlated positively with the MW regime (Pearson's correlation; $r>0.4$, p -value <0.05) (Figure 5B). ME_{b19} was strongly dominated by ASVs enriched in summer events, and included *Cellvibrionales* (26%), and the clades OM60(NOR5) and BD1-7. In addition to the proportion of MW regime, ME_{b19} correlated positively with $CaCO_3$ flux, swimmer flux, SST and Si flux and negatively with unstratified water. Similarly, ME_{b16} , mainly composed of *Alteromonadales* (25%) and *Flavobacteriales* (20%), correlated positively with $CaCO_3$ flux, swimmer flux and distance to the sea ice (Pearson's correlation; $r>0.55$, p -value <0.01), variables that followed a substantial increase in summer after the WWA (Table S1).

4 Discussion

The composition, quantity and interannual variation of sinking particulate matter has been studied at the central HAUSGARTEN station (HGIV) in Fram Strait since 2000 (Soltwedel et al., 2016). The assessment of export fluxes at this site provides a long-term record of biogenic material export and its causes and consequences as well as its key agents (Bauerfeind et al., 2009; Lalande et al., 2011; Lalande et al., 2013; Lalande et al., 2016; Nöthig et al., 2020). In this study, we tested the hypothesis, that the microbial communities involved in particle formation and export are sensitive to interannual changes in the ecosystem state. To investigate this, we studied the seasonality and interannual variation of particle-

associated microbial communities at times of highest organic carbon export (i.e. spring and summer) in the eastern Fram Strait from 2000 to 2012 using the trap-sample bio-archive of the LTER HAUSGARTEN.

4.1 Spring and summer POC flux events reflect environmental changes coupled to seasons

The particle-derived eukaryotic spring core community was strongly dominated by heterotrophic representatives (ASVs of *Dino-Group-I* and *Calanus*), highlighting the contribution of heterotrophic eukaryotic microbes to POC export (Fontanez et al., 2015; Guidi et al., 2016; Boeuf et al., 2019).

The strong connectivity of *Syndiniales* in all three networks concurs with previous network analyses in Fram Strait (Fadeev et al., 2018), the Canadian Arctic (Jacquemot et al., 2022), and other oceanographic regions from the Tara Oceans Expedition (Lima-Mendez et al., 2015). The parasitic lifestyle of *Syndiniales* has been regarded as a significant factor in controlling phytoplankton populations (Guillou et al., 2008; Chaffron et al., 2022; Rizos et al., 2023). The putative parasite-host relationship between *Syndiniales* and *Chaetoceros* has previously been observed in polar regions (Cleary and Durbin, 2016; Clarke et al., 2019) highlights the contribution of *Syndiniales* and dinoflagellates to POC flux through parasitism. Moreover, at the ice margin, *Syndiniales* have been related to spring sea ice communities (*Fragilariopsis*) (Ardyna et al., 2020; Jacquemot et al., 2022), and have been reported to co-occur with *Flavobacteriales* enriched in early bloom conditions in the Fram Strait (Fadeev et al., 2018). In our dataset, diatoms and *Flavobacteriales* were dominant in spring and summer communities, always accompanied by *Syndiniales* (Tables 2, 3), which may indicate that the top-down control of *Syndiniales* in the constitution and transformation of the microbial communities in the sinking particles plays a role in both seasons.

The core ASVs of the copepod *Calanus* also dominated in spring and comprised a considerable fraction of the eukaryotic sequences in sinking particles during spring (6%). Zooplankton in Fram Strait is expected to profit from the onset of the phytoplankton bloom already in spring (Falk-Petersen et al., 2002; Cleary et al., 2017). Species of copepods are important components of summer zooplankton abundance between 100 m and 300 m at the marginal ice zone of Fram Strait where they can reach large abundances in the upper 50 m ($>10,000 \text{ ind m}^{-3}$) also due to copepod nauplii (Kaiser et al., 2021). In addition to copepods, amphipods and chaetognaths were expected to increase in abundance in spring (Ramondenc et al., 2022). However, amphipods and chaetognaths were absent in our dataset. It is likely that the primer pair used in this study, optimized to capture phytoplankton (Metfies et al., 2020), does not capture all zooplankton groups found in the sinking material, while preferentially amplifying some genotypes of copepods, as has been observed for the 18S rDNA V1-V2 hypervariable region (Laakmann et al., 2013).

An ASV assigned to *Micromonas* comprised 3.4% of the spring core community, 4-fold higher than in the core summer

community. Previous studies showed that the picoeukaryote *Micromonas*, a key component of the arctic halocline biomass (Metfies et al., 2016), can be exported to deeper waters via sinking particles, although the explicit mechanisms of export remain unclear (Bachy et al., 2022). *Micromonas* did not exhibit significant interannual variability and was not particularly abundant in our dataset, however we detected *Micromonas* sequences in all samples, where they were likely packed into fecal pellets. Our findings support previous statements about the important contribution of small-cell phytoplankton to carbon export flux in Fram Strait waters (Metfies et al., 2017; Bachy et al., 2022). Future studies should address further export mechanisms of these chlorophytes, as they gain attention as sentinels of ocean warming, due to their species-specific responses to water temperature (Li et al., 2009; Demory et al., 2019; Bachy et al., 2022).

Sea ice concentration reached its maximum in the sediment trap catchment area usually towards the end of the summer, matching the higher contribution of MW regime originating from sea ice melt in summer events. Summer has been characterized by strong stratification during ice melt in the central Arctic Ocean and the Fram Strait (Peralta-Ferriz and Woodgate, 2015; von Appen et al., 2021). Higher sea ice concentration and the resulting MW regime that dominated in summer aided the development and export of diatom blooms over the catchment area of the sediment traps, characteristic of the pre- and post-WWA years (Lalande et al., 2007; Lalande et al., 2013). Thus, Si fluxes were significantly higher during summer (Kruskal-Wallis test; Chi square=7.4, df=1, p -value<0.01), indicating the contribution of diatoms in HPF events. Thus, ASVs of the radiolarian order *Chaunacanthida* and the pelagic diatom *Chaetoceros* dominated in the summer core community (40.2%). Both correlated positively with POC flux (Figure 5A). The correlation of diatoms to carbon export has been previously observed during summer in the North Pacific Ocean with high export pulses at abyssal depths even in silicate-depleted regions (Poff et al., 2021). Diatoms, especially *Chaetoceros*, have also been found to be major contributors to the seasonal export of POC that reaches abyssal depths in the North Pacific (Preston et al., 2020) and in the Southern Ocean (Salter et al., 2012). In general, radiolarians were the most abundant group in our samples, as previously also detected by microscopy in sediment trap samples from 2000-2005 at the same site (Bauerfeind et al., 2009), as well as in other Arctic 18S rRNA gene libraries (Lovejoy and Potvin, 2011). *Chaunacanthida* have also been associated with diatom aggregates of *Chaetoceros* in the Arctic water column (~ 200 m) of Baffin Bay (west coast of Greenland) (Greco et al., 2021), matching our observations of summer assemblages. Moreover, radiolarians are known to contribute to the downward POC flux in summer subsurface waters (Lampitt et al., 2009; Decelle et al., 2013; Fontanez et al., 2015; Guidi et al., 2016; Poff et al., 2021). In addition to foraminifera and pteropods (Ramondenc et al., 2022), acantharians may also be a significant group of sinkers when exported as cysts (Martin et al., 2010). Hence, *Chaunacanthida* might be key contributors to carbon remineralization due to their heterotrophic lifestyle, feeding on zooplankton, phytoplankton and detritus (Lovejoy, 2014), and to carbon export via their association

with sinking particles. Due to the multi-copy nature of the 18S rRNA radiolarian genes, and the presence of multiple nuclei found in *Chaunacanthida* (Decelle and Not, 2015), we cannot rule out that the contribution of these groups may be amplified in our data set (Decelle and Not, 2015). However, if these properties are consistent across samples, the relative differences between samples would be preserved. It is worth noting that this could be mitigated by additional steps to discard PCR artifacts including denoising steps, and to assess and define possible ribotypes in *Chaunacanthida* cells (Decelle et al., 2014).

In contrast, foraminifera are typically exported as empty shells that sink rapidly to the seafloor contributing to CaCO₃ export (Salter et al., 2014; Rembauville et al., 2016; Schiebel et al., 2017) and thus were not detected in the eukaryotic assemblages.

Bacterial communities indicated even stronger seasonal differences between spring and summer than eukaryotes. *Bacilli*, *Bacteroidia*, *Verrucomicrobiae* and *Gammaproteobacteria* were the classes that shifted most between seasons. The spring events were strongly dominated by *Bacilli* taxa known for the absence of a cell wall and being associated with zooplankton i.e. ASVs of *Candidatus* Hepatoplasma and *Mycoplasma* of the class *Entomoplasmatales* (Gallet et al., 2019; Jaspers et al., 2020). *Entomoplasmatales* have been identified as symbionts in meso- and macro-zooplankton (Zbinden and Cambon-Bonavita, 2003; Gallet et al., 2019; Jaspers et al., 2020). Moreover, *Ca. Hepatoplasma* is a genus associated with midgut (hepatopancreas) communities of hadal amphipods (Cheng et al., 2019), and Antarctic krill (Clarke et al., 2019). Families of the dominant *Entomoplasmatales* did not show associations with metazoan families in the third cluster likely due to the low representation of metazoan families in the eukaryotic data set. Neither of these bacterial taxonomic groups were previously identified in such abundance in particle-associated communities in the Fram Strait (Fadeev et al., 2021b), or in sinking particles in other oceanographic regions (Fontanez et al., 2015; Boeuf et al., 2019; Preston et al., 2020; Poff et al., 2021). The strong presence of *Candidatus* Hepatoplasma ASVs as part of the core community in both seasons highlights the presence of zooplankton-associated taxa and the importance of fecal pellets in sinking particles.

Marinifilaceae (Bacteroidales), *Psychromonas* and *Moritella* (Alteromonadales), and the diatom *Thalassiosira* were identified in the earliest spring HPF event in samples with only 8 to 11 h of daylight in March 2001 and 2005. The low availability of sunlight likely prevented the occurrence of an early diatom bloom in March 2001 and 2005, reflected by the low contribution of diatom ASVs (Figure 3). In accordance with this, March 2001 and March 2005 were characterized by a low Si : POC ratio (Table S1), but March 2001 showed the highest swimmer flux of all spring samples, indicating that most of the carbon export might have been driven by an early migration of zooplankton to the sea ice edge at this time. Moreover, resting spores of *Thalassiosira* that became trapped during sea ice formation and a higher proportion of full cells rather than empty frustules likely contributed to the export of carbon in March 2005 (Rembauville et al., 2016), reflected by the low Si:C but high C:N ratios in March 2005. During the transition from winter to spring, *Thalassiosira* usually dominates the water column as well as the sea ice diatom communities at the marginal

ice zone (Bauerfeind et al., 2009; Kauko et al., 2018). Thus, the particle-associated *Bacteroidales* and *Alteromonadales* that characterized the samples from these early events were likely remnants of winter communities.

4.2 Microbial composition of sinking particles reflects changes in oceanographic conditions marked by a warm water anomaly

Beyond seasonal patterns, the eukaryotic community showed significant interannual variability related to a known warm water event in the Arctic (Beszczynska-Möller et al., 2012). Eukaryotic samples clustered into pre-, WWA and post-WWA communities, and particularly the WWA communities were characterized by an overall decrease of diatom sequences (Figure 3). Already with the onset of the increase in temperature at the core of the WSC in 2004 (Beszczynska-Möller et al., 2012), diatom sequences of the dominant taxa of *Chaetoceros* were absent (<1 clr-transformed counts) until 2007 at the end of the WWA period. The diatoms present with the onset of the WWA were mainly assigned to *Thalassiosira* (from August 2004 to May 2006). The peak of the WWA between March 2005 and September 2006 was characterized by a sharp decrease in diatom sequences. Moreover, 2006 was characterized by a change in water column stratification. The ML regime increased between June and August whereas the proportion of MW regime extended over the summer and peaked in October, a pattern that was substantially different from previous years and may have had an effect on primary producers (Figure S11). These findings concur with an expected reduction of the overall export of diatom production in the warmer waters of the WWA (Lalande et al., 2013). During the WWA, the catchment area was mostly characterized by the ML regime, whereas before and after the WWA stronger sea ice presence created a MW regime with stronger stratification (Figure S7). In conjunction with previous results from the water column (Nöthig et al., 2015), our data suggest that the ML regime during the WWA led to the development of a phytoplankton bloom where diatoms were not dominant. This shift in community composition consequently reflected in the composition of particles exported from the surface.

Despite the decline of diatoms during the WWA, we identified a peak of sequences of the sea ice diatom *Melosira* in one sample in September 2006. *Melosira arctica* is a mat-forming diatom attached to sea ice, common in Arctic bottom ice and sub-ice communities (Boetius et al., 2013; Hop et al., 2020). Although *Melosira* has been recorded to form massive ice algal falls in the Central Arctic (Boetius et al., 2013), they have not been commonly observed in sinking particulate matter or at the seafloor in Fram Strait (Soltwedel et al., 2016). Their presence in one HPF sample might be explained by a transient ice floe or advection from ice-covered waters in the catchment area of the sediment trap. In addition, we detected a substantially larger number of fungi sequences in May 2006, specifically of the heterotrophic fungi *Chytridiomycota*. In the Arctic Ocean, *Chytridiomycota* have been shown to associate with diatoms during sea ice melt (Kiliyas et al., 2020). The parasitic and

saprotrophic nature of *Chytridiomycota* in aquatic systems (Ibelings et al., 2004; Gutiérrez et al., 2016) could further explain the sharp decline of diatoms in the spring of May 2006 and highlights potential ecological implications of chytrids for the biological carbon pump.

Sea ice is known to impact carbon export at station HGIV in Fram Strait (Fadeev et al., 2021b; von Appen et al., 2021). Indeed, the WWA and reduced ice export during this period had an effect on the phytoplankton composition, and coincided with reduced HPF-carbon and Si flux during the WWA. Diatoms are important contributors to total POC and Si flux when the cells aggregate and sink directly, but also through the export of resting spores (Salter et al., 2012; Rynearson et al., 2013; Rembauville et al., 2016), empty diatom frustules or packed into fecal pellets, as seen in Fram Strait and the Antarctic Polar Front region (Dagg et al., 2003; Lalande et al., 2011). Previous studies indicated that a ML regime could benefit export as long as diatoms are winners in the system (von Appen et al., 2021). Microscope observations show that diatom aggregation in ice-covered regions in the Arctic Ocean leads to higher carbon export efficiency near the sea ice edge North of Svalbard (Dybwad et al., 2021), as well as stronger vertical microbial connectivity in Fram Strait (Fadeev et al., 2021b), and the Barents Sea (Olli et al., 2019), playing an important role in the export of nutrients to the deep sea. This study and others indicate that diatoms are negatively affected by ocean warming and sea-ice loss in the Arctic, potentially diminishing carbon flux.

Previous studies already revealed a shift in summer phytoplankton from mainly diatom-dominated to more flagellate-dominated communities in the water column of Fram Strait after the WWA (Bauerfeind et al., 2009; Nöthig et al., 2015). Our results based on amplicon sequencing extend these observations to the communities associated with sinking particles collected at the bottom of the epipelagic zone (200 m). Both microscopy and amplicon sequencing methods have their limitations in the quantification of phytoplankton cells (Eiler et al., 2013; Decelle and Not, 2015; Bradley et al., 2016; Fadeev et al., 2021a). However, we find that the observed shifts during the WWA generally agree between methods and with previous observations in the water column. Our data suggest that the transition in phytoplankton composition might have started earlier than previously reported. For instance, we could confirm that *Phaeocystis pouchetii* profited from the WWA and increased in numbers (Nöthig et al., 2015; Metfies et al., 2016), beyond the known increase in abundance during summer (Fadeev et al., 2018). We observed an increase of the flagellate taxa *Phaeocystis*, *Prymnesium* and *Chrysochromulina* already in summer of 2004. Additionally, flagellate ASVs significantly decreased between 2005 and 2006, and less than 5 clr-transformed counts were detected by spring 2006. *Phaeocystis*, *Chrysochromulina* and *Chaetoceros* were consistently dominant again in post-WWA samples. Furthermore, the correlation of flagellates with variables that increased post-WWA; CaCO₃, SST and swimmer flux suggest that flagellates were exported as a result of grazing from swimmers. In addition to *Chaetoceros*, flagellates are and will continue to be important contributors to POC flux in the future (Nöthig et al., 2015). Another documented shift were reports from cell counts of the coccolithophore *Emiliania huxleyi*

that increased already in numbers from 2000 until 2004, after which they were no longer detectable (Nöthig et al., 2015). We did not identify ASVs assigned to *E. huxleyi* in HPF samples, likely due to the reported lower coverage of the coccolithophore order *Isochrydales* by the primer pair applied in our study (Metfies et al., 2020). However, other coccolithophores such as *Gephyrocapsa* were identified in the sinking particles in higher proportions until the peak of the WWA in 2006, and afterwards unassigned ASVs of the *Isochrysidaceae* family remained present in low numbers. Altogether, the changes in the eukaryotic community of sinking particles as detected by amplicon sequencing support the hypothesis of an overall change of the summer phytoplankton community with ocean warming, and especially the occurrence of the WWA event.

Additionally, we identified a bacterial cluster that grouped post-WWA samples of spring events, and was characterized by zooplankton-associated bacterial ASVs assigned to *Ca. Hepatoplasma* (order *Entomoplasmatales*) (Figure 4B). In the time period 2000–2012, both *Calanus* and *Ca. Hepatoplasma* sequences increased substantially after the WWA. Moreover, we observed significant differences in POC flux and CaCO_3 flux between the second and third eukaryotic clusters (*post-hoc* TukeyHSD Tests; *p*-adjusted < 0.01). The significant increase in CaCO_3 flux post-WWA, can be explained by higher pteropod occurrence (Bauerfeind et al., 1997; Bauerfeind et al., 2009). Higher values of POC flux post-WWA coincide with a higher contribution of fecal pellets to POC flux during this period, as indicated by earlier studies (Lalande et al., 2013). Moreover, fecal pellet-derived aggregates can contribute significantly to seasonal changes in POC flux, as observed in the Sargasso Sea, partially due to seasonal differences in zooplankton community composition (Cruz et al., 2021). A recent study of 16 years of zooplankton dynamics in Fram Strait observed that sea ice and temperature dynamics influenced the migration patterns of different swimmers in surface waters (Ramondenc et al., 2022). For instance, an increase of chaetognaths was observed post-WWA and was correlated with temperature changes (Ramondenc et al., 2022). Despite the apparent lack of primer coverage of zooplankton, our observations corroborate the previous findings (Ramondenc et al., 2022), and also agree with an increase in zooplankton abundances reported from the Fram Strait in the years following the WWA (Bauerfeind et al., 2014; Busch et al., 2015; Soltwedel et al., 2016). *Entomoplasmatales* sequences like *Candidatus Hepatoplasma* may thus serve as bacterial indicators of the occurrence of zooplankton and highlight the important role of zooplankton in the origin and modification of sinking particles and their microbial communities in the Arctic Ocean.

4.3 Oceanographic conditions during the WWA induced community shifts leading to changes in carbon export

Co-occurrence network analyses revealed potential associations mostly between diverse eukaryote families of the divisions *Alveolata*, *Hacrobia* and *Stramenopiles*, and bacterial families of

the classes *Gammaproteobacteria*, *Alphaproteobacteria*, *Verrucomicrobiae* and *Bacteroidia*. The latter are a diverse group known to be functionally associated with phytoplankton blooms in the region and to respond to nutrient pulses (Buchan et al., 2014; Wilson et al., 2017; Fadeev et al., 2018; Cardozo-Mino et al., 2021). The relatively high organic matter content of the particles during the HPF events explains the large number of associations that involved copiotrophic taxa of *Gammaproteobacteria*, *Alphaproteobacteria* and *Verrucomicrobia* in all three networks.

We expected the putative associations between bacteria and eukaryotes to change qualitatively before, during and after the WWA, because different phytoplankton communities composed the particles. In addition, more bacteria-to-bacteria associations (e.g. *Gammaproteobacteria* and *Alphaproteobacteria*) were observed during the WWA, and between eukaryotes in the post-WWA period. Altogether, the changes described here indicate a perturbation of the microbial network structure and a substantial change of particle composition, colonization and degradation of the particles at the time of the WWA.

The overall reduction in POC and PON fluxes in HPF events during the WWA have likely been caused by a phytoplankton shift initiated in 2004 and a concurrent change in the size of the particles (Henson et al., 2019). The likely higher retention of small buoyant particles of flagellates at the surface may have allowed for a different set of bacterial taxa to colonize the particles and allowed for more retention of carbon at the surface (Vernet et al., 2017). Compared to the other clusters, the second cluster showed more numerous co-occurrences between *Gammaproteobacteria* and *Alphaproteobacteria* families. This further indicates a shift in the bacterial network of the WWA. *Gammaproteobacteria* and *Alphaproteobacteria* are well known for their large catalogue of hydrolytic enzymes needed to degrade organic matter from algal exudates and phytodetritus thus relevant in the remineralization of primary production products (Buchan et al., 2014; Teeling et al., 2016). Changes in particle composition may also lead to changes in other properties including size and porosity (Bach et al., 2019). Carbon remineralization is mainly controlled by the residence time of the particles in the water column and exposure to ecto-enzymatic hydrolysis, microbial respiration and grazing from zooplankton (Iversen and Ploug, 2010). Moreover, phytoplankton community structure might considerably influence particle remineralization rates (Bach et al., 2019). Therefore, quantification of carbon remineralization and microbial respiration rates along with particle composition is needed for a detailed evaluation of the implications of the retention system in the upper ocean. Such combined analyses are essential to evaluate whether particle size and microbial community structure (Guidi et al., 2009) can serve as a proxy for estimating carbon export efficiency.

In order to investigate in more detail changes in the composition of the particles that could reflect in changes in vertical particle fluxes, we identified putative associations between bacterial and eukaryotic families specific to the WWA. For instance, associations between heterotrophic pico- and nano-plankton families of MAST-1, MAST-9 and MAST-12 affiliation, and other heterotrophs including the divisions *Filosa-Sarcomonadea* and *Telonemia* with bacterial taxa assigned to the orders

Oceanospirillales, *Alteromonadales* and *Rhodobacterales* increased during the WWA. Approaching the peak of the WWA in 2005 and 2006, we observed a notable increase in the sequence abundances of ASVs of copiotrophic genera of *Gammaproteobacteria* and *Alphaproteobacteria* like *Alcanivorax*, *Marinobacter* and *Sulfitobacter*. These groups have not been detected as dominant taxa in surveys of free-living and particle-associated bacteria in previous studies of Fram Strait (Wilson et al., 2017; Fadeev et al., 2018; Fadeev et al., 2021b). *Rhodobacterales* represent a bacterial order known to be associated with the warmer and saltier conditions of surface Atlantic waters (Cardozo-Mino et al., 2021). Within the *Rhodobacterales*, *Sulfitobacter* and *Amylibacter* are among potential indicator taxa of Atlantic origin including the Barents Sea (Aalto et al., 2022). The presence of these taxa may thus represent a microbial Atlantification phenomenon.

Marinobacter, *Sulfitobacter* and *Alcanivorax* are part of the dominant community of hydrocarbon-degrading bacteria in the sub-Arctic regions of the Faroe-Shetland Channel, impacted by oil and gas industry (Angelova et al., 2021). *Alcanivorax* may be involved in the degradation of hydrocarbons in marine POM, such as *n*-alkanes potentially produced by dinoflagellates of the WWA, e.g. *Gymnodinium catenatum*, which has been isolated from drifting sea ice north of Svalbard (Green et al., 2004; de Sousa et al., 2019), or oils derived from zooplankton (Yoshimura and Hama, 2012; Daase et al., 2014). Species of *Marinobacter* and *Sulfitobacter* are known to associate with eukaryotes (Chernikova et al., 2020) and to get enriched in DOM of unfixed sediment trap samples (Fontanez et al., 2015). For instance, *Marinobacter* has shown specific attachment to diatom cells of *Thalassiosira weissflogii* (Gärdes et al., 2010), and coccolithophorids including *Emiliana huxleyi* (Green et al., 2015). However, here *Marinobacter* showed possible associations with ASVs assigned to MAST-9C, *Protospa-lineage* and *Chaunacanthida* during the WWA. Although coccolithophorids, the diatom *Thalassiosira* and *Marinobacter* increased during the WWA, their lack of association in the network analysis might be indicative of a disturbance effect. In contrast, heterotrophic protists like MAST-9, MAST-1, and MAST-12 played a significant role in the construction of the network, highlighting their significance during the WWA. The presence of bacteria not usually associated with phytoplankton blooms and the associations unique to the WWA period further supports an altered, potentially more retentive system. This may contribute to the overall decrease in carbon export during this time, in addition to the observed decrease in fecal pellet production and particle volume during the WWA (Lalande et al., 2013).

5 Conclusions

We integrated 12 years of observations of sinking particle fluxes with molecular analyses of archived sediment trap samples, and with remote sensing and modelled data from a high-resolution Lagrangian back-tracking model. In addition to seasonal differences in microbial communities, we identified significant changes in the

microbial communities associated with sinking particles over this time period. These were mainly driven by surface oceanographic conditions in the area, most importantly by the presence/absence of sea ice, and by marked changes during a WWA episode between 2005 and 2007. The WWA period was characterized by low ice concentration, higher temperatures, and unstratified waters, favoring the development of microbial communities and specific networks indicative of a retention system with higher proportions of flagellates and copiotrophic bacteria.

The general agreement of our results with previous microscopic observations suggest that bio-archives of mercury-chloride preserved sediment trap samples can be used to assess baseline shifts and address changes in the microbial composition of sinking particles over long time scales. This offers high-throughput and high-resolution insights into community dynamics and networks. The future Arctic Ocean will become warmer and sea ice cover will continue to decline. Our observations expand previous reports, indicating that changes in sea ice cover and hydrography will have major impacts on the efficiency of POC export, by altering phytoplankton composition and associated microbial networks. To better predict consequences of these changes for the biological carbon pump, future studies should address Arctic microbial community dynamics at a higher temporal resolution and from surface to seafloor.

Data availability statement

The datasets presented in this study can be found in online repositories. The names of the repository/repositories and accession number(s) can be found below: <https://www.ebi.ac.uk/ena>, PRJEB43086 <https://www.ebi.ac.uk/ena>, PRJEB43576.

Author contributions

IS, CB and AB conceived and designed the study. KM and IS conducted Illumina sequencing of the samples. E-MN provided background and data for the sediment trap time series. SR determined the distance to the sea ice edge from remote sensing data products. CW obtained the catchment area from a backward Lagrangian model. IS, TK and CW provided weighted means of sea ice concentration, SST and chlorophyll *a*. MC-M analyzed the data and wrote the manuscript with guidance from CB, IS, E-MN and AB. All authors critically revised the manuscript and gave their approval of the submitted version.

Funding

This project has received funding from the European Research Council (ERC) Advanced Grant ABYSS (no. 294757) to AB. MC-M

was funded by the Hector Fellow Academy. Additional funding was provided by the Max Planck Society and the Helmholtz Association. This work was conducted in the framework of the HGF Infrastructure Program FRAM of the Alfred-Wegener-Institute Helmholtz Center for Polar and Marine Research.

Acknowledgments

We thank the captains and crew of RV Polarstern and RV Maria S. Merian expeditions to Fram Strait from 2000 to 2013, as well as the chief scientists and scientific crews. We thank Eduard Bauerfeind for the design, deployment and recovery of sediment traps in Fram Strait. Nadine Knüppel, Christiane Lorenzen, Sandra Murawski, Liz Bonk and many student helpers and apprentices are greatly acknowledged for their support on board and in the laboratory. We thank Theresa Hargesheimer for processing samples for molecular analyses. Halina Tegetmeyer performed sequencing of the bacterial samples and Swantje Rogge of eukaryotic samples. We thank the reviewers and the editor for their valuable comments and suggestions.

References

- Aalto, N. J., Schweitzer, H. D., Krsmanovic, S., Campbell, K., and Bernstein, H. C. (2022). Diversity and selection of surface marine microbiomes in the Atlantic-influenced Arctic. *Front. Microbiol.* 13. doi: 10.3389/fmicb.2022.892634
- Allredge, A. L., and Silver, M. W. (1988). Characteristics, dynamics and significance of marine snow. *Prog. Oceanogr.* 20, 41–82. doi: 10.1016/0079-6611(88)90053-5
- Angelova, A. G., Berx, B., Bresnan, E., Joye, S. B., Free, A., and Gutierrez, T. (2021). Inter- and intra-annual bacterioplankton community patterns in a deepwater Sub-Arctic region: persistent high background abundance of putative oil degraders. *MBio* 12, e03701–e03720. doi: 10.1128/mBio.03701-20
- Ardyna, M., Mundy, C. J., Mayot, N., Matthes, L. C., Oziel, L., Horvat, C., et al. (2020). Under-ice phytoplankton blooms: shedding light on the “invisible” part of Arctic primary production. *Front. Mar. Sci.* 7. doi: 10.3389/fmars.2020.608032
- Arrigo, K. R., Perovich, D. K., Pickart, R. S., Brown, Z. W., Van Dijken, G. L., Lowry, K. E., et al. (2012). Massive phytoplankton blooms under arctic sea ice. *Science* 336, 1408–1408. doi: 10.1126/science.1215065
- Azam, F., and Malfatti, F. (2007). Microbial structuring of marine ecosystems. *Nat. Rev. Microbiol.* 5, 782–791. doi: 10.1038/nrmicro1747
- Bach, L. T., Boxhammer, T., Larsen, A., Hildebrandt, N., Schulz, K. G., and Riebesell, U. (2016). Influence of plankton community structure on the sinking velocity of marine aggregates. *Global Biogeochem. Cycles* 30, 1145–1165. doi: 10.1029/2019GB006256
- Bach, L. T., Stange, P., Taucher, J., Achterberg, E. P., Alguero-Muñoz, M., Horn, H., et al. (2019). The influence of plankton community structure on sinking velocity and remineralization rate of marine aggregates. *Global Biogeochem. Cycles* 33, 971–994. doi: 10.1029/2019GB006256
- Bachy, C., Sudek, L., Choi, C. J., Eckmann, C. A., Nöthig, E.-M., Metfies, K., et al. (2022). Phytoplankton surveys in the Arctic fram strait demonstrate the tiny eukaryotic alga micromonas and other picoprasinophytes contribute to deep sea export. *Microorganism* 10(5), 961. doi: 10.3390/microorganisms10050961
- Bauerfeind, E., Garrity, C., Krumbholz, M., Ramseier, R. O., and Voß, M. (1997). Seasonal variability of sediment trap collections in the Northeast Water Polynya. Part 2. Biochemical and microscopic composition of sedimenting matter. *J. Mar. Syst.* 10, 371–389. doi: 10.1016/S0924-7963(96)00069-3
- Bauerfeind, E., Nöthig, E. M., Beszczynska, A., Fahl, K., Kaleschke, L., Kreker, K., et al. (2009). Particle sedimentation patterns in the eastern Fram Strait during 2000–2005: results from the Arctic long-term observatory HAUSGARTEN. *Deep. Res. Part I Oceanogr. Res. Pap.* 56, 1471–1487. doi: 10.1016/j.dsr.2009.04.011
- Bauerfeind, E., Nöthig, E.-M., Pauls, B., Kraft, A., and Beszczynska-Möller, A. (2014). Variability in pteropod sedimentation and corresponding aragonite flux at the Arctic deep-sea long-term observatory HAUSGARTEN in the eastern fram strait from 2000 to 2009. *J. Mar. Syst.* 132, 95–105. doi: 10.1016/j.jmarsys.2013.12.006
- Beszczynska-Moeller, A., Woodgate, R. A., Lee, C., Melling, H., and Karcher, M. (2011). A synthesis of exchanges through the main oceanic gateways to the Arctic Ocean. *Oceanography* 24, 82–99. doi: 10.5670/oceanog.2011.59
- Beszczynska-Möller, A., Fahrback, E., Schauer, U., and Hansen, E. (2012). Variability in Atlantic water temperature and transport at the entrance to the Arctic Ocean 1997–2010. *ICES J. Mar. Sci.* 69, 852–863. doi: 10.1093/icesjms/fss056
- Bodungen, B. V., Wunsch, M., and Fürderer, H. (1991). Sampling and analysis of suspended and sinking particles in the northern North Atlantic. *Washingt. DC Am. Geophys. Union Geophys. Monogr. Ser.* 63, 47–56. doi: 10.1029/GM063p0047
- Boetius, A., Albrecht, S., Bakker, K., Bienhold, C., Felden, J., Fernández-Méndez, M., et al. (2013). Export of algal biomass from the melting arctic sea ice. *Science* 339, 1430–1432. doi: 10.1126/science.1231346
- Boeuf, D., Edwards, B. R., Eppley, J. M., Hu, S. K., Poff, K. E., Romano, A. E., et al. (2019). Biological composition and microbial dynamics of sinking particulate organic matter at abyssal depths in the oligotrophic open ocean. *Proc. Natl. Acad. Sci. U. S. A.* 116, 11824–11832. doi: 10.1073/pnas.1903080116
- Bostock, M., Patrick, E., Russell, K., Tarr, G., and Tarr, M. G. (2016). *edgebundleR: circle plot with bundled edges*. Available at: <https://github.com/garhtarr/edgebundleR>.
- Bradley, I. M., Pinto, A. J., and Guest, J. S. (2016). Design and evaluation of illumina MiSeq-compatible, 18S rRNA gene-specific primers for improved characterization of mixed phototrophic communities. *Appl. Environ. Microbiol.* 82, 5878–5891. doi: 10.1128/AEM.01630-16
- Buchan, A., LeClerc, G. R., Gulvik, C. A., and González, J. M. (2014). Master recyclers: features and functions of bacteria associated with phytoplankton blooms. *Nat. Rev. Microbiol.* 12, 686–698. doi: 10.1038/nrmicro3326
- Buesseler, K. O., and Boyd, P. W. (2009). Shedding light on processes that control particle export and flux attenuation in the twilight zone of the open ocean. *Limnol. Oceanogr.* 54, 1210–1232. doi: 10.4319/lo.2009.54.4.1210
- Busch, K., Bauerfeind, E., and Nöthig, E. M. (2015). Pteropod sedimentation patterns in different water depths observed with moored sediment traps over a 4-year period at the LTER station HAUSGARTEN in Eastern Fram Strait. *Polar Biol.* 38, 845–859. doi: 10.1007/s00300-015-1644-9
- Callahan, B. J., McMurdie, P. J., Rosen, M. J., Han, A. W., Johnson, A. J. A., and Holmes, S. P. (2016). DADA2: high-resolution sample inference from illumina amplicon data. *Nat. Methods* 13, 581–583. doi: 10.1038/nmeth.3869
- Cardozo-Mino, M. G., Fadeev, E., Salman-Carvalho, V., and Boetius, A. (2021). Spatial distribution of Arctic bacterioplankton abundance is linked to distinct water masses and summertime phytoplankton bloom dynamics (Fram Strait, 79°N). *Front. Microbiol.* 12. doi: 10.3389/fmicb.2021.658803

Conflict of interest

The authors declare that the research was conducted in the absence of any commercial or financial relationships that could be construed as a potential conflict of interest.

Publisher's note

All claims expressed in this article are solely those of the authors and do not necessarily represent those of their affiliated organizations, or those of the publisher, the editors and the reviewers. Any product that may be evaluated in this article, or claim that may be made by its manufacturer, is not guaranteed or endorsed by the publisher.

Supplementary material

The Supplementary Material for this article can be found online at: <https://www.frontiersin.org/articles/10.3389/fmars.2023.1173384/full#supplementary-material>

- Chaffron, S., Delage, E., Budinich, M., Vintache, D., Henry, N., Nef, C., et al. (2022). Environmental vulnerability of the global ocean epipelagic plankton community intertactome. *Sci. Adv.* 7, eabg1921. doi: 10.1126/sciadv.abg1921
- Cheng, X., Wang, Y., Li, J., Yan, G., and He, L. (2019). Comparative analysis of the gut microbial communities between two dominant amphipods from the challenger deep, Mariana trench. *Deep Sea Res. Part I Oceanogr. Res. Pap.* 151, 103081. doi: 10.1016/j.dsr.2019.103081
- Chernikova, T. N., Bargiela, R., Toshchakov, S. V., Shivaraman, V., Lunev, E. A., Yakimov, M. M., et al. (2020). Hydrocarbon-degrading bacteria alcanivorax and marinobacter associated with microalgae *Pavlova lutheri* and *Nannochloropsis oculata*. *Front. Microbiol.* 11. doi: 10.3389/fmicb.2020.572931
- Clarke, L. J., Bestley, S., Bissett, A., and Deagle, B. E. (2019). A globally distributed syndiniales parasite dominates the southern ocean micro-eukaryote community near the sea-ice edge. *ISME J.* 13, 734–737. doi: 10.1038/s41396-018-0306-7
- Claustre, H., Legendre, L., Boyd, P. W., and Levy, M. (2021). The oceans' biological carbon pumps: framework for a research observational community approach. *Front. Mar. Sci.* 8. doi: 10.3389/fmars.2021.780052
- Cleary, A. C., and Durbin, E. G. (2016). Unexpected prevalence of parasite 18S rDNA sequences in winter among Antarctic marine protists. *J. Plankton Res.* 38, 401–417. doi: 10.1093/plankt/fbw005
- Cleary, A. C., Søreide, J. E., Freese, D., Niehoff, B., and Gabrielsen, T. M. (2017). Feeding by calanus glacialis in a high arctic fjord: potential seasonal importance of alternative prey. *ICES J. Mar. Sci.* 74, 1937–1946. doi: 10.1093/icesjms/fix106
- Cram, J. A., Xia, L. C., Needham, D. M., Sachdeva, R., Sun, F., and Fuhrman, J. A. (2015). Cross-depth analysis of marine bacterial networks suggests downward propagation of temporal changes. *ISME J.* 9, 2573–2586. doi: 10.1038/ismej.2015.76
- Cruz, B. N., Brozak, S., and Neuer, S. (2021). Microscopy and DNA-based characterization of sinking particles at the Bermuda Atlantic time-series study station point to zooplankton mediation of particle flux. *Limnol. Oceanogr.* 66, 3697–3713. doi: 10.1002/lno.11910
- Csardi, G., and Nepusz, T. (2006) *The igraph software package for complex network research*. Available at: <http://www.necsi.edu/events/icc6/papers/c1602a3c126ba822d0bc4293371c.pdf>.
- Daase, M., Varpe, Ø., and Falk-Petersen, S. (2014). Non-consumptive mortality in copepods: occurrence of calanus spp. carcasses in the Arctic ocean during winter. *J. Plankton Res.* 36, 129–144. doi: 10.1093/plankt/fbt079
- Dagg, M. J., Urban-Rich, J., and Peterson, J. O. (2003). The potential contribution of fecal pellets from large copepods to the flux of biogenic silica and particulate organic carbon in the Antarctic polar front region near 170°W. *Deep Sea Res. Part II Top. Stud. Oceanogr.* 50, 675–691. doi: 10.1016/S0967-0645(02)00590-8
- Dai, A., Luo, D., Song, M., and Liu, J. (2019). Arctic Amplification is caused by sea-ice loss under increasing CO₂. *Nat. Commun.* 10, 121. doi: 10.1038/s41467-018-07954-9
- Datta, M. S., Sliwerska, E., Gore, J., Polz, M. F., and Cordero, O. X. (2016). Microbial interactions lead to rapid micro-scale successions on model marine particles. *Nat. Commun.* 7, 1–7. doi: 10.1038/ncomms11965
- Decelle, J., Martin, P., Paborstava, K., Pond, D. W., Tarling, G., Mahé, F., et al. (2013). Diversity, ecology and biogeochemistry of cyst-forming acantharia (Radiolaria) in the oceans. *PLoS One* 8, e53598. doi: 10.1371/journal.pone.0053598
- Decelle, J., and Not, F. (2015). Acantharia. *Princeton NJ ELS*. doi: 10.1002/9780470015902.a0002102.pub2
- Decelle, J., Romac, S., Sasaki, E., Not, F., and Mahé, F. (2014). Intracellular diversity of the V4 and V9 regions of the 18S rRNA in marine protists (Radiolarians) assessed by high-throughput sequencing. *PLoS One* 9, e104297. doi: 10.1371/journal.pone.0104297
- De La Rocha, C. L., and Passow, U. (2007). Factors influencing the sinking of POC and the efficiency of the biological carbon pump. *Deep. Res. Part II Top. Stud. Oceanogr.* 54, 639–658. doi: 10.1016/j.dsr2.2007.01.004
- Demory, D., Baudoux, A.-C., Monier, A., Simon, N., Six, C., Ge, P., et al. (2019). Picoeukaryotes of the micromonas genus: sentinels of a warming ocean. *ISME J.* 13, 132–146. doi: 10.1038/s41396-018-0248-0
- de Sousa, A. G. G., Tomasino, M. P., Duarte, P., Fernández-Méndez, M., Assmy, P., Ribeiro, H., et al. (2019). Diversity and composition of pelagic prokaryotic and protist communities in a thin Arctic sea-ice regime. *Microb. Ecol.* 78, 388–408. doi: 10.1007/s00248-018-01314-2
- Deuser, W. G., Muller-Karger, F. E., and Hemleben, C. (1988). Temporal variations of particle fluxes in the deep subtropical and tropical north Atlantic: eulerian versus Lagrangian effects. *J. Geophys. Res. Ocean.* 93, 6857–6862. doi: 10.1029/JC093iC06p06857
- Diepenbroek, M., Glöckner, F. O., Grobe, P., Güntsch, A., Huber, R., König-Ries, B., et al. (2014). "Towards an integrated biodiversity and ecological research data management and archiving platform: the German federation for the curation of biological data (GFBio)," in *Informatik 2014*. Eds. E. Plödereder, L. Grunke, E. Schneider and D. Ull (Bonn: Gesellschaft für Informatik e.V.), Stuttgart, 1711–1721.
- Ducklow, H. W., Steinberg, D. K., and Buesseler, K. O. (2001). Upper ocean carbon export and the biological pump. *Oceanography* 14, 50–58. doi: 10.5670/oceanog.2001.06
- Duran-Pinedo, A. E., Paster, B., Teles, R., and Frias-Lopez, J. (2011). Correlation network analysis applied to complex biofilm communities. *PLoS One* 6, e28438. doi: 10.1371/journal.pone.0028438
- Dybwad, C., Assmy, P., Olsen, L. M., Peeken, I., Nikolopoulos, A., Krumpfen, T., et al. (2021). Carbon export in the seasonal Sea ice zone north of Svalbard from winter to late summer. *Front. Mar. Sci.* 7. doi: 10.3389/fmars.2020.525800
- Eiler, A., Drakare, S., Bertilsson, S., Pernthaler, J., Peura, S., Rofner, C., et al. (2013). Unveiling distribution patterns of freshwater phytoplankton by a next generation sequencing based approach. *PLoS One* 8, e53516. doi: 10.1371/journal.pone.0053516
- Elwood, H. J., Olsen, G. J., and Sogin, M. L. (1985). The small-subunit ribosomal RNA gene sequences from the hypotrichous ciliates oxytricha nova and styloynchia pustulata. *Mol. Biol. Evol.* 2, 399–410. doi: 10.1093/oxfordjournals.molbev.a040362
- Ezraty, R., Girard-Ardhuin, F., Piollé, J., Kaleschke, L., and Heygster, G. (2007). *Arctic And Antarctic Sea ice concentration and Arctic Sea ice drift estimated from special sensor microwave imager data. 2.1* (Brest, France and University of Bremen, Germany: Department d'Océanographie Physique et Spatiale, IFREMER).
- Fadeev, E., Cardozo-Mino, M. G., Rapp, J. Z., Bienhold, C., Salter, I., Salman-Carvalho, V., et al. (2021a). Comparison of two 16S rRNA primers (V3–V4 and V4–V5) for studies of Arctic microbial communities. *Front. Microbiol.* 12. doi: 10.3389/fmicb.2021.637526/full
- Fadeev, E., Rogge, A., Ramondenc, S., Nöthig, E.-M., Wekerle, C., Bienhold, C., et al. (2021b). Sea Ice presence is linked to higher carbon export and vertical microbial connectivity in the Eurasian Arctic ocean. *Commun. Biol.* 4, 1255. doi: 10.1038/s42003-021-02776-w
- Fadeev, E., Salter, I., Schourup-Kristensen, V., Nöthig, E. M., Metfies, K., Engel, A., et al. (2018). Microbial communities in the east and west fram strait during sea ice melting season. *Front. Mar. Sci.* 5. doi: 10.3389/fmars.2018.00429
- Falk-Petersen, S., Dahl, T. M., Scott, C. L., Sargent, J. R., Gulliksen, B., Kwasniewski, S., et al. (2002). Lipid biomarkers and trophic linkages between ctenophores and copepods in Svalbard waters. *Mar. Ecol. Prog. Ser.* 227, 187–194. doi: 10.3354/meps227187
- Fontanez, K. M., Eppley, J. M., Samo, T. J., Karl, D. M., and DeLong, E. F. (2015). Microbial community structure and function on sinking particles in the north pacific subtropical gyre. *Front. Microbiol.* 6. doi: 10.3389/fmicb.2015.00469
- Gallet, A., Koubbi, P., Léger, N., Scheifler, M., Ruiz-Rodriguez, M., Suzuki, M. T., et al. (2019). Low-diversity bacterial microbiota in southern ocean representatives of lanternfish genera electrona, protomyctophum and gymnoscopelus (family myctophidae). *PLoS One* 14, e022615. doi: 10.1371/journal.pone.0226159
- Gärdes, A., Kaeppl, E., Shehzad, A., Seebah, S., Teeling, H., Yarza, P., et al. (2010). Complete genome sequence of marinobacter adhaerens type strain (HP15), a diatom-interacting marine microorganism. *Stand. Genomic Sci.* 3, 97–107. doi: 10.4056/sigs.922139
- Gibbons, S. M., Caporaso, J. G., Pirrung, M., Field, D., Knight, R., and Gilbert, J. A. (2013). Evidence for a persistent microbial seed bank throughout the global ocean. *Proc. Natl. Acad. Sci. U. S. A.* 110, 4651–4655. doi: 10.1073/pnas.1217767110
- Grabowski, E., Letelier, R. M., Laws, E. A., and Karl, D. M. (2019). Coupling carbon and energy fluxes in the north pacific subtropical gyre. *Nat. Commun.* 10, 1–9. doi: 10.1038/s41467-019-09772-z
- Greco, M., Morard, R., and Kucera, M. (2021). Single-cell metabarcoding reveals biotic interactions of the Arctic calcifier neogloboquadrina pachyderma with the eukaryotic pelagic community. *J. Plankton Res.* 43, 113–125. doi: 10.1093/plankt/fbab015
- Green, D. H., Echavarrri-Bravo, V., Brennan, D., and Hart, M. C. (2015). Bacterial diversity associated with the coccolithophorid algae *Emiliania huxleyi* and *Coccolithus pelagicus* f. *braarudii*. *BioMed. Res. Int.* 2015, 194540. doi: 10.1155/2015/194540
- Green, D. H., Llewellyn, L. E., Negri, A. P., Blackburn, S. I., and Bolch, C. J. S. (2004). Phylogenetic and functional diversity of the cultivate bacterial community associated with the paralytic shellfish poisoning dinoflagellate gymnodinium catenatum. *FEMS Microbiol. Ecol.* 47, 345–357. doi: 10.1016/S0168-6496(03)00298-8
- Grosfeld, K., Treffeisen, R., Asseng, J., Bartsch, A., Bräuer, B., Fritsch, B., et al. (2016). Online sea-ice knowledge and data platform. *Polarforschung* 85, 143–155. doi: 10.2312/polfor.2016.011
- Grossart, H.-P., Kjørboe, T., Tang, K., and Ploug, H. (2003). Bacterial colonization of particles: growth and interactions. *Appl. Environ. Microbiol.* 69, 3500–3509. doi: 10.1128/aem.69.6.3500-3509.2003
- Guidi, L., Chaffron, S., Bittner, L., Eveillard, D., Larhlmi, A., Roux, S., et al. (2016). Plankton networks driving carbon export in the oligotrophic ocean. *Nature* 532, 465–470. doi: 10.1038/nature16942
- Guidi, L., Stemann, L., Jackson, G. A., Ibanez, F., Claustre, H., Legendre, L., et al. (2009). Effects of phytoplankton community on production, size and export of large aggregates: a world-ocean analysis. *Limnol. Oceanogr.* 54, 1951–1963. doi: 10.4319/lo.2009.54.6.1951
- Guillou, L., Bachar, D., Audic, S., Bass, D., Berney, C., Bittner, L., et al. (2013). The protist ribosomal reference database (PR2): a catalog of unicellular eukaryote small Sub-unit rRNA sequences with curated taxonomy. *Nucleic Acids Res.* 41, D597–D604. doi: 10.1093/nar/gks1160
- Guillou, L., Viprey, M., Chambouvet, A., Welsh, R. M., Kirkham, A. R., Massana, R., et al. (2008). Widespread occurrence and genetic diversity of marine parasitoids belonging to syndiniales (Alveolata). *Environ. Microbiol.* 10, 3349–3365. doi: 10.1111/j.1462-2920.2008.01731.x
- Gutiérrez, M. H., Jara, A. M., and Pantoja, S. (2016). Fungal parasites infect marine diatoms in the upwelling ecosystem of the Humboldt current system off central Chile. *Environ. Microbiol.* 18, 1646–1653. doi: 10.1111/1462-2920.13257

- Harrison, P. W., Ahamed, A., Aslam, R., Alako, B. T. F., Burgin, J., Buso, N., et al. (2021). The European nucleotide archive in 2020. *Nucleic Acids Res.* 49, D82–D85. doi: 10.1093/nar/gkaa1028
- Henson, S., Le Moigne, F., and Giering, S. (2019). Drivers of carbon export efficiency in the global ocean. *Global Biogeochem. Cycles* 33, 891–903. doi: 10.1029/2018GB006158
- Hop, H., Assmy, P., Wold, A., Sundfjord, A., Daase, M., Duarte, P., et al. (2019). Pelagic ecosystem characteristics across the Atlantic water boundary current from rjppfjorden, Svalbard, to the Arctic ocean during summer, (2010–2014). *Front. Mar. Sci.* 6. doi: 10.3389/fmars.2019.00181
- Hop, H., Vihtakari, M., Bluhm, B. A., Assmy, P., Poulin, M., Gradinger, R., et al. (2020). Changes in Sea-ice protist diversity with declining Sea ice in the Arctic ocean from the 1980s to 2010s. *Front. Mar. Sci.* 7. doi: 10.3389/fmars.2020.00243
- Hsieh, T. C., Ma, K. H., and Chao, A. (2016). iNEXT: an R package for rarefaction and extrapolation of species diversity (Hill numbers). *Methods Ecol. Evol.* 7, 1451–1456. doi: 10.1111/2041-210X.12613
- Ibelings, B. W., De Bruin, A., Kagami, M., Rijkeboer, M., Brehm, M., and Van Donk, E. (2004). Host parasite interactions between freshwater phytoplankton and chytrid fungi (chytridiomycota). *J. Phycol.* 40, 437–453. doi: 10.1111/j.1529-8817.2004.03117.x
- Iversen, M. H. (2023). Carbon export in the ocean: a biologist's perspective. *Ann. Rev. Mar. Sci.* 15, 357–381. doi: 10.1146/annurev-marine-032122-035153
- Iversen, M. H., and Ploug, H. (2010). Ballast minerals and the sinking carbon flux in the ocean: carbon-specific respiration rates and sinking velocity of marine snow aggregates. *Biogeochemistry* 7, 2613–2624. doi: 10.5194/bg-7-2613-2010
- Jacquemot, L., Vigneron, A., Tremblay, J.-É., and Lovejoy, C. (2022). Contrasting sea ice conditions shape microbial food webs in Hudson bay (Canadian Arctic). *ISME Commun.* 2, 104. doi: 10.1038/s43705-022-00192-7
- Jaspers, C., Weiland-Bräuer, N., Rühlmann, M. C., Baines, J. F., Schmitz, R. A., and Reusch, T. B. H. (2020). Differences in the microbiota of native and non-indigenous gelatinous zooplankton organisms in a low saline environment. *Sci. Total Environ.* 734, 139471. doi: 10.1016/j.scitotenv.2020.139471
- Jiao, N., Herndl, G. J., Hansell, D. A., Benner, R., Kattner, G., Wilhelm, S. W., et al. (2010). Microbial production of recalcitrant dissolved organic matter: long-term carbon storage in the global ocean. *Nat. Rev. Microbiol.* 8, 593–599. doi: 10.1038/nrmicro2386
- Kaiser, P., Hagen, W., von Appen, W.-J., Niehoff, B., Hildebrandt, N., and Auel, H. (2021). Effects of a submesoscale oceanographic filament on zooplankton dynamics in the Arctic marginal ice zone. *Front. Mar. Sci.* 8. doi: 10.3389/fmars.2021.625395
- Kauko, H. M., Olsen, L. M., Duarte, P., Peeken, I., Granskog, M. A., Johnsen, G., et al. (2018). Algal colonization of young Arctic Sea ice in spring. *Front. Mar. Sci.* 5. doi: 10.3389/fmars.2018.00199
- Kilius, E. S., Junges, L., Šupraha, L., Leonard, G., Metfies, K., and Richards, T. A. (2020). Chytrid fungi distribution and co-occurrence with diatoms correlate with sea ice melt in the Arctic ocean. *Commun. Biol.* 3, 183. doi: 10.1038/s42003-020-0891-7
- Klindworth, A., Pruesse, E., Schweer, T., Peplies, J., Quast, C., Horn, M., et al. (2013). Evaluation of general 16S ribosomal RNA gene PCR primers for classical and next-generation sequencing-based diversity studies. *Nucleic Acids Res.* 41, e1. doi: 10.1093/nar/gks808
- Kruppen, T., Belter, H. J., Boetius, A., Damm, E., Haas, C., Hendricks, S., et al. (2019). Arctic Warming interrupts the transpolar drift and affects long-range transport of sea ice and ice-rafted matter. *Sci. Rep.* 9, 5459. doi: 10.1038/s41598-019-41456-y
- Kurtz, Z. D., Müller, C. L., Miraldi, E. R., Littman, D. R., Blaser, M. J., and Bonneau, R. A. (2015). Sparse and compositionally robust inference of microbial ecological networks. *PLoS Comput. Biol.* 11, e1004226. doi: 10.1371/journal.pcbi.1004226
- Laakmann, S., Gerdt, G., Erler, R., Kneibelsberger, T., Martínez Arbizu, P., and Raupach, M. J. (2013). Comparison of molecular species identification for north Sea calanoid copepods (Crustacea) using proteome fingerprints and DNA sequences. *Mol. Ecol. Resour.* 13, 862–876. doi: 10.1111/1755-0998.12139
- Lalande, C., Bauerfeind, E., and Nöthig, E. M. (2011). Downward particulate organic carbon export at high temporal resolution in the eastern fram strait: influence of Atlantic water on flux composition. *Mar. Ecol. Prog. Ser.* 440, 127–136. doi: 10.3354/meps09385
- Lalande, C., Bauerfeind, E., Nöthig, E. M., and Beszczynska-Möller, A. (2013). Impact of a warm anomaly on export fluxes of biogenic matter in the eastern fram strait. *Prog. Oceanogr.* 109, 70–77. doi: 10.1016/j.pocean.2012.09.006
- Lalande, C., Grebmeier, J. M., Wassmann, P., Cooper, L. W., Flint, M. V., and Sergeeva, V. M. (2007). Export fluxes of biogenic matter in the presence and absence of seasonal sea ice cover in the chukchi Sea. *Cont. Shelf Res.* 27, 2051–2065. doi: 10.1016/j.csr.2007.05.005
- Lalande, C., Nöthig, E.-M., Bauerfeind, E., Hardge, K., Beszczynska-Möller, A., and Fahl, K. (2016). Lateral supply and downward export of particulate matter from upper waters to the seafloor in the deep eastern fram strait. *Deep Sea Res. Part I Oceanogr. Res. Pap.* 114, 78–89. doi: 10.1016/j.dsr.2016.04.014
- Lalande, C., Nöthig, E. M., Somavilla, R., Bauerfeind, E., Shevchenko, V., and Okolodkov, Y. (2014). Variability in under-ice export fluxes of biogenic matter in the Arctic ocean. *Global Biogeochem. Cycles* 28, 571–583. doi: 10.1002/2013GB004735
- Lampitt, R. S., Salter, I., and Johns, D. (2009). Radiolaria: major exporters of organic carbon to the deep ocean. *Global Biogeochem. Cycles* 23, GB1010. doi: 10.1029/2008GB003221
- Langfelder, P., and Horvath, S. (2008). WGCNA: an R package for weighted correlation network analysis. *BMC Bioinf.* 9, 559. doi: 10.1186/1471-2105-9-559
- Lannuzel, D., Tedesco, L., van Leeuwe, M., Campbell, K., Flores, H., Delille, B., et al. (2020). The future of Arctic sea-ice biogeochemistry and ice-associated ecosystems. *Nat. Clim. Change* 10, 983–992. doi: 10.1038/s41558-020-00940-4
- Leu, E., Søreide, J. E., Hessen, D. O., Falk-Petersen, S., and Berge, J. (2011). Consequences of changing sea-ice cover for primary and secondary producers in the European Arctic shelf seas: timing, quantity, and quality. *Prog. Oceanogr.* 90, 18–32. doi: 10.1016/j.pocean.2011.02.004
- Lewis, K. M., Van Dijken, G. L., and Arrigo, K. R. (2020). Changes in phytoplankton concentration now drive increased Arctic ocean primary production. *Science* 369, 198–202. doi: 10.1126/science.aay8380
- Li, W. K. W., McLaughlin, F. A., Lovejoy, C., and Carmack, E. C. (2009). Smallest algae thrive as the arctic ocean freshens. *Science* 326, 539. doi: 10.1126/science.1179798
- Lima-Mendez, G., Faust, K., Henry, N., Decelle, J., Colin, S., Carcillo, F., et al. (2015). Determinants of community structure in the global plankton interactome. *Science* 22, 348(6237). doi: 10.1126/science.1262073
- Liu, Y., Blain, S., Crispi, O., Rembauville, M., and Obernosterer, I. (2020). Seasonal dynamics of prokaryotes and their associations with diatoms in the southern ocean as revealed by an autonomous sampler. *Environ. Microbiol.* 22, 3968–3984. doi: 10.1111/1462-2920.15184
- Love, M. I., Huber, W., and Anders, S. (2014). Moderated estimation of fold change and dispersion for RNA-seq data with DESeq2. *Genome Biol.* 15, 554. doi: 10.1186/s13059-014-0550-8
- Lovejoy, C. (2014). Changing views of Arctic protists (marine microbial eukaryotes) in a changing Arctic. *Acta Protozool.* 53, 91–100. doi: 10.4467/16890027AP.14.009.1446
- Lovejoy, C., and Potvin, M. (2011). Microbial eukaryotic distribution in a dynamic Beaufort Sea and the Arctic ocean. *J. Plankton Res.* 33, 431–444. doi: 10.1093/plankt/fbq124
- Martin, M. (2011). Cutadapt removes adapter sequences from high-throughput sequencing reads. *EMBnet Journal* 17, 10. doi: 10.14806/ej.17.1.200
- Martin, P., Allen, J. T., Cooper, M. J., Johns, D. G., Lampitt, R. S., Sanders, R., et al. (2010). Sedimentation of acantharian cysts in the Iceland basin: strontium as a ballast for deep ocean particle flux, and implications for acantharian reproductive strategies. *Limnol. Oceanogr.* 55, 604–614. doi: 10.4319/lo.2010.55.2.0604
- McMurdie, P. J., and Holmes, S. (2013). Phyloseq: an R package for reproducible interactive analysis and graphics of microbiome census data. *PLoS One* 8, e61217. doi: 10.1371/journal.pone.0061217
- Mestre, M., Ruiz-González, C., Logares, R., Duarte, C. M., Gasol, J. M., and Sala, M. M. (2018). Sinking particles promote vertical connectivity in the ocean microbiome. *Proc. Natl. Acad. Sci. U. S. A.* 115, E6799–E6807. doi: 10.1073/pnas.1802470115
- Metfies, K., Bauerfeind, E., Wolf, C., Sprong, P., Frickenhaus, S., Kaleschke, L., et al. (2017). Protist communities in moored long-term sediment traps (Fram strait, arctic)-preservation with mercury chloride allows for PCR-based molecular genetic analyses. *Front. Mar. Sci.* 4. doi: 10.3389/fmars.2017.00301
- Metfies, K., Hessel, J., Klenk, R., Petersen, W., Wiltshire, K. H., and Kraberg, A. (2020). Uncovering the intricacies of microbial community dynamics at helgoland roads at the end of a spring bloom using automated sampling and 18S meta-barcoding. *PLoS One* 15, e023392. doi: 10.1371/journal.pone.0233921
- Metfies, K., von Appen, W.-J., Kilius, E., Nicolaus, A., and Nöthig, E.-M. (2016). Biogeography and photosynthetic biomass of arctic marine pico-eukaryotes during summer of the record sea ice minimum 2012. *PLoS One* 11, e014851. doi: 10.1371/journal.pone.0148512
- Nöthig, E. M., Bracher, A., Engel, A., Metfies, K., Niehoff, B., Peeken, I., et al. (2015). Summertime plankton ecology in fram strait—a compilation of long-and short-term observations. *Polar Res.* 34, 23349. doi: 10.3402/polar.v34.23349
- Nöthig, E. M., Ramondenc, S., Haas, A., Hehemann, L., Walter, A., Bracher, A., et al. (2020). Summertime chlorophyll a and particulate organic carbon standing stocks in surface waters of the fram strait and the Arctic ocean, (1991–2015). *Front. Mar. Sci.* 7. doi: 10.3389/fmars.2020.00350
- Oksanen, J., Blanchet, F. G., Kindt, R., Legendre, P., Minchin, P. R., O'hara, R. B., et al. (2013). “Ackage ‘vegan’,” in *Community ecology package, version 2.9*. Available at: <http://CRAN.R-project.org/package=vegan>
- Olli, K., Halvorsen, E., Vernet, M., Lavrentyev, P. J., Franzè, G., Sanz-Martin, M., et al. (2019). Food web functions and interactions during spring and summer in the Arctic water inflow region: investigated through inverse modeling. *Front. Mar. Sci.* 6. doi: 10.3389/fmars.2019.00244
- Peng, G., and Meier, W. N. (2018). Temporal and regional variability of Arctic sea-ice coverage from satellite data. *Ann. Glaciol.* 59, 191–200. doi: 10.1017/aog.2017.32
- Peralta-Ferriz, C., and Woodgate, R. A. (2015). Seasonal and interannual variability of pan-Arctic surface mixed layer properties from 1979 to 2012 from hydrographic data, and the dominance of stratification for multiyear mixed layer depth shoaling. *Prog. Oceanogr.* 134, 19–53. doi: 10.1016/j.pocean.2014.12.005

- Poff, K. E., Leu, A. O., Eppley, J. M., Karl, D. M., and DeLong, E. F. (2021). Microbial dynamics of elevated carbon flux in the open ocean's abyss. *Proc. Natl. Acad. Sci. U. S. A.* 118(4), e2018269118. doi: 10.1073/pnas.2018269118
- Preston, C. M., Durkin, C. A., and Yamahara, K. M. (2020). DNA Metabarcoding reveals organisms contributing to particulate matter flux to abyssal depths in the north east pacific ocean. *Deep. Res. Part II Top. Stud. Oceanogr.* 173, 104708. doi: 10.1016/j.dsr2.2019.104708
- Quast, C., Pruesse, E., Yilmaz, P., Gerken, J., Schweer, T., Yarza, P., et al. (2013). The SILVA ribosomal RNA gene database project: improved data processing and web-based tools. *Nucleic Acids Res.* 41, D590–D596. doi: 10.1093/nar/gks1219
- Ramondenc, S., Nöthig, E.-M., Hufnagel, L., Bauerfeind, E., Busch, K., Knüppel, N., et al. (2022). Effects of atlantification and changing sea-ice dynamics on zooplankton community structure and carbon flux between 2000 and 2016 in the eastern fram strait. *Limnol. Oceanogr.* doi: 10.1002/lno.12192
- Rantanen, M., Karpechko, A. Y., Lipponen, A., Nordling, K., Hyvärinen, O., Ruosteenoja, K., et al. (2022). The Arctic has warmed nearly four times faster than the globe since 1979. *Commun. Earth Environ.* 3, 168. doi: 10.1038/s43247-022-00498-3
- Rapp, J. Z., Fernández-Méndez, M., Bienhold, C., and Boetius, A. (2018). Effects of ice-algal aggregate export on the connectivity of bacterial communities in the central Arctic ocean. *Front. Microbiol.* 9. doi: 10.3389/fmicb.2018.01035
- Rembauville, M., Manno, C., Tarling, G. A., Blain, S., and Salter, I. (2016). Strong contribution of diatom resting spores to deep-sea carbon transfer in naturally iron-fertilized waters downstream of south Georgia. *Deep. Res. Part I Oceanogr. Res. Pap.* 115, 22–35. doi: 10.1016/j.dsr.2016.05.002
- Rizos, I., Debeljak, P., Finet, T., Klein, D., Ayata, S.-D., Not, F., et al. (2023). Beyond the limits of the unassigned protist microbiome: inferring large-scale spatio-temporal patterns of syndiniales marine parasites. *ISME Commun.* 3, 16. doi: 10.1038/s43705-022-00203-7
- Ruiz-González, C., Mestre, M., Estrada, M., Sebastián, M., Salazar, G., Agusti, S., et al. (2020). Major imprint of surface plankton on deep ocean prokaryotic structure and activity. *Mol. Ecol.* 29, 1820–1838. doi: 10.1111/mec.15454
- Rynearson, T. A., Richardson, K., Lampitt, R. S., Sieracki, M. E., Poulton, A. J., Lyngsgaard, M. M., et al. (2013). Major contribution of diatom resting spores to vertical flux in the sub-polar north Atlantic. *Deep. Res. Part I Oceanogr. Res. Pap.* 82, 60–71. doi: 10.1016/j.dsr.2013.07.013
- Salter, I., Kemp, A. E. S., Moore, C. M., Lampitt, R. S., Wolff, G. A., and Holtvoeth, J. (2012). Diatom resting spore ecology drives enhanced carbon export from a naturally iron-fertilized bloom in the southern ocean. *Global Biogeochem. Cycles* 26, GB1014. doi: 10.1029/2010GB003977
- Salter, I., Schiebel, R., Ziveri, P., Movellan, A., Lampitt, R., and Wolff, G. A. (2014). Carbonate counter pump stimulated by natural iron fertilization in the polar frontal zone. *Nat. Geosci.* 7, 885–889. doi: 10.1038/ngeo2285
- Schiebel, R., Spielhagen, R. F., Garnier, J., Hagemann, J., Howa, H., Jentzen, A., et al. (2017). Modern planktic foraminifers in the high-latitude ocean. *Mar. Micropaleontol.* 136, 1–13. doi: 10.1016/j.marmicro.2017.08.004
- Schröter, F., Havermans, C., Kraft, A., Knüppel, N., Beszczynska-Möller, A., Bauerfeind, E., et al. (2019). Pelagic amphipods in the eastern fram strait with continuing presence of themisto compressa based on sediment trap time series. *Front. Mar. Sci.* 6. doi: 10.3389/fmars.2019.00311
- Simon, M., Grossart, H. P., Schweitzer, B., and Ploug, H. (2002). Microbial ecology of organic aggregates in aquatic ecosystems. *Aquat. Microb. Ecol.* 28, 175–211. doi: 10.3354/ame028175
- Soltwedel, T., Bauerfeind, E., Bergmann, M., Bracher, A., Budaeva, N., Busch, K., et al. (2016). Natural variability or anthropogenically-induced variation? insights from 15 years of multidisciplinary observations at the arctic marine LTER site HAUSGARTEN. *Ecol. Indic.* 65, 89–102. doi: 10.1016/j.ecolind.2015.10.001
- Stroeve, J., and Notz, D. (2018). Changing state of Arctic sea ice across all seasons. *Environ. Res. Lett.* 13, 103001. doi: 10.1088/1748-9326/aade56
- Teeling, H., Fuchs, B. M., Bennis, C. M., Krüger, K., Chafee, M., Kappelmann, L., et al. (2016). Recurring patterns in bacterioplankton dynamics during coastal spring algae blooms. *Elife* 5, e11888. doi: 10.7554/eLife.11888
- Thiele, S., Fuchs, B. M., Amann, R., and Iversen, M. H. (2015). Colonization in the photic zone and subsequent changes during sinking determine bacterial community composition in marine snow. *Appl. Environ. Microbiol.* 81, 1463–1471. doi: 10.1128/AEM.02570-14
- Turner, J. T. (2015). Zooplankton fecal pellets, marine snow, phytodetritus and the ocean's biological pump. *Prog. Oceanogr.* 130, 205–248. doi: 10.1016/j.pcean.2014.08.005
- Vernet, M., Richardson, T. L., Metfies, K., Nöthig, E.-M., and Peeken, I. (2017). Models of plankton community changes during a warm water anomaly in Arctic waters show altered trophic pathways with minimal changes in carbon export. *Front. Mar. Sci.* 4. doi: 10.3389/fmars.2017.00160
- von Appen, W.-J., Waite, A. M., Bergmann, M., Bienhold, C., Boebel, O., Bracher, A., et al. (2021). Sea-Ice derived meltwater stratification slows the biological carbon pump: results from continuous observations. *Nat. Commun.* 12, 7309. doi: 10.1038/s41467-021-26943-z
- Waite, A. M., Stemmann, L., Guidi, L., Calil, P. H. R., Hogg, A. M. C., Feng, M., et al. (2016). The wineglass effect shapes particle export to the deep ocean in mesoscale eddies. *Geophys. Res. Lett.* 43, 9791–9800. doi: 10.1002/2015GL066463
- Walczowski, W., Beszczynska-Möller, A., Wiczorek, P., Merchel, M., and Grynczel, A. (2017). Oceanographic observations in the Nordic Sea and fram strait in 2016 under the IO PAN long-term monitoring program AREX. *Oceanologia* 59, 187–194. doi: 10.1016/j.ocean.2016.12.003
- Waniek, J. J., Schulz-Bull, D. E., Blanz, T., Prien, R. D., Oschlies, A., and Müller, T. J. (2005). Interannual variability of deep water particle flux in relation to production and lateral sources in the northeast Atlantic. *Deep Sea Res. Part I Oceanogr. Res. Pap.* 52, 33–50. doi: 10.1016/j.dsr.2004.08.008
- Wassmann, P., and Reigstad, M. (2011). Future Arctic ocean seasonal ice zones and implications for pelagic-benthic coupling. *Oceanography* 24, 220–231. doi: 10.5670/oceanog.2011.74
- Wekerle, C., Krumpen, T., Dinter, T., von Appen, W. J., Iversen, M. H., and Salter, I. (2018). Properties of sediment trap catchment areas in fram strait: results from Lagrangian modeling and remote sensing. *Front. Mar. Sci.* 9. doi: 10.3389/fmars.2018.00407
- Wekerle, C., Wang, Q., von Appen, W. J., Danilov, S., Schourup-Kristensen, V., and Jung, T. (2017). Eddy-resolving simulation of the Atlantic water circulation in the fram strait with focus on the seasonal cycle. *J. Geophys. Res. Ocean.* 122, 8385–8405. doi: 10.1002/2017JC012974
- Weydmann, A., Carstensen, J., Goszczko, I., Dmoch, K., Olszewska, A., and Kwasniewski, S. (2014). Shift towards the dominance of boreal species in the Arctic: inter-annual and spatial zooplankton variability in the West spitsbergen current. *Mar. Ecol. Prog. Ser.* 501, 41–52. doi: 10.3354/meps10694
- Wickham, H., Averick, M., Bryan, J., Chang, W., McGowan, L., François, R., et al. (2019). Welcome to the tidyverse. *J. Open Source Software* 4, 1686. doi: 10.21105/joss.01686
- Wiedmann, I., Ershova, E., Bluhm, B. A., Nöthig, E.-M., Gradinger, R. R., Kosobokova, K., et al. (2020). What feeds the benthos in the Arctic basins? assembling a carbon budget for the deep Arctic ocean. *Front. Mar. Sci.* 7. doi: 10.3389/fmars.2020.00224
- Wietz, M., Metfies, K., Bienhold, C., Wolf, C., Janssen, F., Salter, I., et al. (2022). Impact of preservation method and storage period on ribosomal metabarcoding of marine microbes: implications for remote automated samplings. *Front. Microbiol.* 13. doi: 10.3389/fmicb.2022.999925
- Wilson, J. M., Litvin, S. Y., and Beman, J. M. (2018). Microbial community networks associated with variations in community respiration rates during upwelling in nearshore Monterey bay, California. *Environ. Microbiol. Rep.* 10, 272–282. doi: 10.1111/1758-2229.12635
- Wilson, B., Müller, O., Nordmann, E. L., Seuthe, L., Bratbak, G., and Øvreås, L. (2017). Changes in marine prokaryote composition with season and depth over an Arctic polar year. *Front. Mar. Sci.* 4. doi: 10.3389/fmars.2017.00095
- Yilmaz, P., Kottmann, R., Field, D., Knight, R., Cole, J. R., Amaral-Zettler, L., et al. (2011). Minimum information about a marker gene sequence (MIMARKS) and minimum information about any (x) sequence (MIxS) specifications. *Nat. Biotechnol.* 29, 415–420. doi: 10.1038/nbt.1823
- Yoshimura, K., and Hama, T. (2012). Degradation and dissolution of zooplanktonic organic matter and lipids in early diagenesis. *J. Oceanogr.* 68, 205–214. doi: 10.1007/s10872-011-0091-7
- Zbinden, M., and Cambon-Bonavita, M.-A. (2003). Occurrence of deferribacterales and entomoplasmatales in the deep-sea alvinocarid shrimp rimicaris exoculata gut. *FEMS Microbiol. Ecol.* 46, 23–30. doi: 10.1016/S0168-6496(03)00176-4